

Table 2. List of DRG Genes Selectively Upregulated at Day 7 and Day 14 After Nerve Root Ligation

Gene Symbol	Gene Name	Accession No.	Functional Categorization	Day 2	Day 7	Day 14
S100a4	S100 calcium-binding protein A4	NM_012618	Cell cycle	1.7	3.2	2.6
Pycard	Apoptosis-associated speck-like protein containing a CARD	NM_172322	Cell cycle	1.7	2.4	2.1
Plk2	Polo-like kinase 2	AF136583	Cell cycle	1.4	2.1	2.7
Slc12a1	Solute carrier family 12, member 1	NM_019134	Channels/transporter	1.5	5.6	5.4
Aqp3	Aquaporin 3	L35108	Channels/transporter	1.3	2.7	2.9
Ctss	Cathepsin S	NM_017320	Enzyme/metabolism	1.7	4.9	3.5
Dpp6	Dipeptidylpeptidase 6	M76426	Enzyme/metabolism	1.1	4.5	4.4
Adn	Adipsin	S73894	Enzyme/metabolism	1.6	3.9	4.4
Mmp2	Matrix metalloproteinase 2	U65656	Enzyme/metabolism	1.2	3.0	2.6
Ctsk	Cathepsin K	AF010306	Enzyme/metabolism	1.4	2.7	2.4
Cnp1	Cyclic nucleotide phosphodiesterase 1	L16532	Enzyme/metabolism	1.1	2.6	2.4
Slpi	Secretory leukocyte peptidase inhibitor	AF151982	Enzyme/metabolism	1.6	2.6	2.3
Plat	Plasminogen activator, tissue	NM_013151	Enzyme/metabolism	1.5	2.5	2.6
Pld1	Phospholipase D1	U69550	Enzyme/metabolism	1.4	2.4	2.2
Cp	Ceruloplasmin	NM_012532	Enzyme/metabolism	1.2	2.4	2.2
Hspa2	Heat shock protein 2	NM_021863	Enzyme/metabolism	1.2	2.4	2.1
Xdh	Xanthine dehydrogenase	NM_017154	Enzyme/metabolism	1.4	2.4	2.4
Dnah7	Dynein, axonemal, heavy polypeptide 7	D26498	Enzyme/metabolism	1.6	2.2	2.1
Mmp10	Matrix metalloproteinase 10	M65253	Enzyme/metabolism	1.1	2.2	2.4
Ugdh	UDP-glucose dehydrogenase	AB013732	Enzyme/metabolism	1.7	2.1	2.3
Fap	Fibroblast activation protein	NM_138850	Enzyme/metabolism	1.4	2.0	2.0
Entpd2	Ectonucleoside triphosphate diphosphohydrolase 2	AF276940	Enzyme/metabolism	1.0	2.0	2.2
Mdk	Midkine	AB025023	Growth factors/cytokines	1.3	2.3	2.1
Igf1	Insulin-like growth factor I	M81184	Growth factors/cytokines	1.5	2.3	2.6
Tgfb1	Transforming growth factor, beta induced	AF305713	Growth factors/cytokines	1.5	2.2	2.0
C1qb	Complement component 1, q subcomponent, beta polypeptide	NM_019262	Immune	1.9	3.5	2.4
Cxcl9	Chemokine (C-X-C motif) ligand 9	NM_145672	Immune	1.0	3.5	3.5
Cfh	Complement component factor H	NM_130409	Immune	1.5	2.7	2.8
Cd86	Cd86 antigen	D50558	Immune	1.8	2.1	2.4
Apod	Apolipoprotein D	NM_012777	Signal transduction	1.7	4.7	3.3
Lgp85	85 kDa sialoglycoprotein	D10587	Signal transduction	1.7	3.1	2.6
Gng11	Guanine nucleotide binding protein (G protein), γ 11	AF257110	Signal transduction	1.6	3.1	3.1
Gfra1	Glial cell line derived neurotrophic factor family receptor α	NM_012959	Signal transduction	1.9	3.1	2.3
Cd53	CD53 antigen	NM_012523	Signal transduction	1.7	2.8	2.3
Ramp1	Receptor (calcitonin) activity modifying protein 1	AB042887	Signal transduction	1.4	2.7	2.5
Csrp2	Cysteine and glycine-rich protein 2	U44948	Signal transduction	1.2	2.6	2.6
Ogfr	Opioid growth factor receptor	AF156878	Signal transduction	1.4	2.4	2.3
Vcam1	Vascular cell adhesion molecule 1	NM_012889	Signal transduction	1.7	2.2	2.1
Sostdc1	Uterine sensitization-associated gene 1 protein	NM_153737	Signal transduction	0.8	2.2	2.4
Sifn3	Schlafen 3	AF168795	Signal transduction	1.7	2.1	2.1
Col3a1	Collagen, type III, α 1	M21354	Structure	1.8	4.0	2.9
Serpinh1	Serine (or cysteine) proteinase inhibitor, clade H, member 1	NM_017173	Structure	1.9	2.6	2.4
Lum	Lumican	X84039	Structure	1.6	2.4	2.3
Col5a1	Collagen, type V, α 1	AF272662	Structure	1.5	2.3	2.5
Vil2	Villin 2	X67788	Structure	1.8	2.3	2.1
Col1a1	Collagen, type 1, α 1	Z78279	Structure	1.2	2.2	2.0
DLP2	Dynein-like protein 2	D26493	Structure	1.5	2.1	2.2
Apobec1	Apolipoprotein B editing complex 1	NM_012907	Transcription/translation	1.6	3.3	3.0
Mafk	v-maf musculoaponeurotic fibrosarcoma oncogene family, protein B	U56241	Transcription/translation	1.4	2.4	2.4
Nupr1	Nuclear protein 1	AF014503	Transcription/translation	1.1	2.3	2.0
H3f3b	H3 histone, family 3B	X73683	Transcription/translation	1.6	2.2	2.0
Irf1	Interferon regulatory factor 1	NM_012591	Transcription/translation	1.7	2.1	2.0
Meox2	Mesenchyme homeo box 2	NM_017149	Transcription/translation	1.5	2.1	2.4
Btg1	B-cell translocation gene 1, anti-proliferative	L26268	Transcription/translation	1.7	2.1	2.9
Lhx2	LIM homeobox protein 2	L06804	Transcription/translation	1.6	2.0	2.4
Drcf5	Developmentally-regulated cardiac factor	U95001	Unknown	1.6	2.5	2.7

The average Cy5/Cyt 3 ratio of gene in triplicate microarray experiments were calculated. Genes showing the ratio of two or more at day 7 and day 14, but not day 2 were listed.

cluster composed of the day-2 DRG samples. Subsequently, we identified 89 genes, including 16 genes that were upregulated only at day 2 after nerve root ligation, 56 genes that were upregulated at days 7 and 14, and another 17 genes that showed consistent upregulation

from day 2 to day 21. These findings indicate the involvement of distinct sets of genes in the early phase (day 2) and the later phase (day 7 and later) of development of lumbar radiculopathy. The number of upregulated genes was larger in the midphase than in the early phase, cor-

Table 3. List of DRG Genes Continuously Upregulated From Day 2 to Day 21 After Nerve Root Ligation

Gene symbol	Gene Name	Accession No.	Functional Categorization	Day 2	Day 7	Day 14	Day 21
Kif11	Kinesin family member 11	AF035955	Cell cycle	2.5	3.2	3.0	2.1
Lyz	Lysozyme	NM_012771	Enzyme/metabolism	2.1	6.2	5.0	3.6
Crabp2	Cellular retinoic acid binding protein 2	U23407	Enzyme/metabolism	3.1	3.3	3.0	2.1
Enpp3	Ectonucleotide pyrophosphatase/ phosphodiesterase 3	NM_019370	Enzyme/metabolism	2.7	3.8	4.8	2.8
Reg3g	Regenerating islet-derived 3γ	L20869	Enzyme/metabolism	2.7	2.2	4.9	2.7
A2m	α-2-macroglobulin	NM_012488	Enzyme/metabolism	5.1	11.6	10.8	2.3
Ifitm2	Interferon induced transmembrane protein 2 (1-8D)	AF164040	Immune	2.0	3.1	2.1	2.1
Gbp2	Guanylate nucleotide binding protein 2	M80367	Immune	3.1	3.9	4.1	2.1
Ifitm3	Interferon induced transmembrane protein 3	AF164039	Immune	2.3	3.3	2.6	2.3
Fcgr2b	Fc receptor, IgG, low affinity IIb	X73371	Immune	4.4	3.1	2.8	2.4
Gpnmb	Glycoprotein (transmembrane) nmb	AF184983	Signal transduction	2.3	3.6	4.8	2.9
Cdh4	Cadherin 4	D86742	Signal transduction	2.0	3.4	2.6	2.0
Vim	Vimentin	X62952	Structure	2.7	4.8	2.8	2.2
Thbs4	Thrombospondin 4	X89963	Structure	2.1	7.2	5.8	2.3
Cthrc1	Collagen triple helix repeat containing 1	NM_172333	Structure	4.7	8.7	10.4	2.5
Fn1	Fibronectin 1	NM_019143	Structure	2.8	3.3	3.1	2.1
Col18a1	Procollagen, type XVIII, α1	AF189709	Structure	3.5	6.8	5.4	2.4

The average Cy5/Cyt 3 ratio of gene in triplicate microarray experiments were calculated. Genes showing the ratio of 2 or more continuously from day 2 to day 21 were listed.

responding to the painful behavior of the nerve-ligated rats which peaked during the midphase.¹⁵

Functional categorization revealed dominantly up-regulated gene categories in each group. They included transcription/translation, signal transduction, and enzyme/metabolism in the early phase and enzyme/metabolism, signal transduction, transcription/translation, and structure in the midphase. Consistent with our findings, genes categorized into enzyme/metabolism, signal transduction, transcription/translation, and structure were also dominantly upregulated in the dorsal horn of the spinal cord 7 and 14 days after nerve root ligation in a rat model.⁴

Based on clustering analysis, we classified genes into the early phase, midphase, and continuous group. In this regard, genes upregulated on day 14 or later may be classified as the late phase. We found only 2 genes in this group, including EGF-like domain, multiple 3 and coxsackie virus and adenovirus receptor.

Genes upregulated in the DRG with nerve root ligation may contribute to a variety of biologic processes including pain signaling, inflammation, and regeneration of the injured nerve. Of these, the genes involved in pain

signaling and inflammation may serve as potential targets of pharmacological or genetic approach for lumbar radiculopathy. This idea is well exemplified by prostaglandin-endoperoxide synthase 2, which is upregulated in the early phase of our model. Prostaglandin-endoperoxide synthase 2 is known as cyclooxygenase 2 (COX-2). Involvement of COX-2 in acute pain and inflammation has been established.^{18,19} Also, therapeutic efficacy of a selective COX-2 inhibitor has been demonstrated in rat radiculopathy models.^{20,21} Besides prostag-

Table 5. Real-Time Quantitative PCR Analysis of Day 7 DRG

Gene Name	Probe No.*	Ligation	Sham
Apolipoprotein D	Rn00562832_m1	12.0**	1.0
CD53 antigen	Rn00560957_m1	4.7	0.9
Aquaporin 3	Rn00581754_m1	64.0	0.8
Receptor (calcitonin) activity modifying protein 1	Rn00581278_m1	2.7	0.5
Secretory leukocyte peptidase inhibitor	Rn00670378_m1	15.9	0.7
Plasminogen activator, tissue	Rn00565767_m1	3.3	0.9
Heat shock protein 2	Rn00434069_s1	3.0	1.2
Xanthine dehydrogenase	Rn00567654_m1	3.9	0.9
V-maf musculoaponeurotic fibrosarcoma oncogene family, protein B	Rn00709456_s1	2.7	1.3
Opioid growth factor receptor	Rn00584280_m1	1.6	1.0
Collagen, type V, α1	Rn00593170_m1	2.6	1.0
Uterine sensitization- associated gene 1 protein	Rn00596672_m1	2.7	0.9
Polo-like kinase 2	Rn00582709_m1	3.2	1.1
cd86 antigen	Rn00571654_m1	6.4	0.9
UDP-glucose dehydrogenase	Rn00580047_m1	4.4	1.1
B-cell translocation gene 1, anti-proliferative	Rn00820872_g1	3.8	0.8
Ectonucleoside triphosphate diphosphohydrolase 2	Rn00596961_m1	3.3	1.0

*The catalog no. of TaqMan probes (Applied Biosystems).

**The mean relative expression values of three root-ligated rats and sham-operated rats were described, respectively.

Table 4. Percentage of Genes Classified by Functional Category

	Early	Mid	Consistent
Cell cycle	6	5	6
Channels/transporters	6	4	0
Enzyme/metabolism	13	31	29
Growth factors/cytokines	6	5	0
Immune	6	7	24
Signal transduction	19	20	12
Structure	0	13	29
Synaptic	6	0	0
Transcription/translation	31	15	0
Unknown	6	2	0

landin-endoperoxide synthase 2, calcium-activated chloride channel may contribute to pain signaling in lumbar radiculopathy, because calcium-activated chloride current²² has been shown to increase after axotomy in rats. In contrast to these molecules, heme oxygenase (decycling) 1 serves cytoprotective actions in several pathologic conditions including inflammation²³ and sciatic nerve injury.²⁴ Thus, there may be therapeutic benefits with heme oxygenase (decycling) 1 in lumbar radiculopathy. Among 56 genes that were upregulated in the midphase, the involvement of cathepsin S in neuropathic pain has been recently reported.^{25,26} Given the fact that inhibition of cathepsin S led to reversal of neuropathic pain after peripheral nerve injury, this approach can also be applied to neuropathic condition subsequent to lumbar radiculopathy.

The present study has several limitations, including—(i) imperfect validity of microarray results (94%), (ii) placement of sham-operated controls only at 1 time point (day 7), and (iii) lack of immunohistochemical or *in situ* hybridization studies that reveals cell types expressing genes upregulated. Nevertheless, this is the first comprehensive analysis of gene expression in the DRG adjacent to nerve root ligation. The present study serves as the initial step toward identification of therapeutic targets for lumbar radiculopathy and development of molecularly targeted therapy.

■ Key Points

- DNA array analysis was conducted for the DRG adjacent to the injured nerve root in a rat lumbar radiculopathy model.
- Of 7793 genes analyzed, 16 genes were upregulated in the DRG on day 2 after nerve root ligation (early phase group), 56 genes on both days 7 and 14 (midphase group), and 17 genes from day 2 to day 21 (continuous group).
- Dominantly upregulated gene categories were transcription/translation in the early phase group, enzyme/metabolism in the midphase group, and structure in the continuous group.

References

1. Hasue M. Pain and the nerve root: an interdisciplinary approach. *Spine* 1993;18:2053–305.
2. Winkelstein BA, DeLeo JA. Mechanical thresholds for initiation and persistence of pain following nerve root injury: mechanical and chemical contributions at injury. *J Biomech Eng* 2004;126:258–63.
3. Song XJ, Vizcarra C, Xu DS, et al. Hyperalgesia and neural excitability following injuries to central and peripheral branches of axons and somata of dorsal root ganglion neurons. *J Neurophysiol* 2003;89:2185–93.
4. Lacroix-Fralish ML, Tawfik VL, Tanga FY, et al. Differential spinal cord gene expression in rodent models of radicular and neuropathic pain. *Anesthesiology* 2006;104:1283–92.
5. Reilly SC, Cossins AR, Quinn JP, et al. Discovering genes: the use of microarrays and laser capture microdissection in pain research. *Brain Res Brain Res Rev* 2004;46:225–33.
6. Zhang X, Xiao HS. Gene array analysis to determine the components of neuropathic pain signaling. *Curr Opin Mol Ther* 2005;7:532–7.
7. Costigan M, Befort K, Karchewski L, et al. Replicate high-density rat genome oligonucleotide microarrays reveal hundreds of regulated genes in the dorsal root ganglion after peripheral nerve injury. *BMC Neurosci* 2002;3:16.
8. Xiao HS, Huang QH, Zhang FX, et al. Identification of gene expression profile of dorsal root ganglion in the rat peripheral axotomy model of neuropathic pain. *Proc Natl Acad Sci USA* 2002;99:8360–5.
9. Valder CR, Liu JJ, Song YH, et al. Coupling gene chip analyses and rat genetic variances in identifying potential target genes that may contribute to neuropathic allodynia development. *J Neurochem* 2003;87:560–73.
10. Rodriguez Parkitna J, Korostynski M, Kaminska-Chowanic D, et al. Comparison of gene expression profiles in neuropathic and inflammatory pain. *J Physiol Pharmacol* 2006;57:401–14.
11. Ko J, Na DS, Lee YH, et al. cDNA microarray analysis of the differential gene expression in the neuropathic pain and electroacupuncture treatment models. *J Biochem Mol Biol* 2002;35:420–7.
12. Sun H, Xu J, Della Penna KB, et al. Dorsal horn-enriched genes identified by DNA microarray, *in situ* hybridization and immunohistochemistry. *BMC Neurosci* 2002;3:11.
13. Yang L, Zhang FX, Huang F, et al. Peripheral nerve injury induces trans-synaptic modification of channels, receptors and signal pathways in rat dorsal spinal cord. *Eur J Neurosci* 2004;19:871–83.
14. LaCroix-Fralish ML, Tawfik VL, Spratt KF, et al. Sex differences in lumbar spinal cord gene expression following experimental lumbar radiculopathy. *J Mol Neurosci* 2006;30:283–95.
15. Kirita T, Takebayashi T, Mizuno S, et al. Electrophysiologic changes in dorsal root ganglion neurons and behavioral changes in a lumbar radiculopathy model. *Spine* 2007;32:E65–72.
16. Hashizume H, DeLeo JA, Colburn RW, et al. Spinal glial activation and cytokine expression after lumbar root injury in the rat. *Spine* 2000;25:1206–17.
17. Abe M, Kurihara T, Han W, et al. Changes in expression of voltage-dependent ion channel subunits in dorsal root ganglia of rats with radicular injury and pain. *Spine* 2002;27:1517–24; discussion 25.
18. Lee Y, Rodriguez C, Dionne RA. The role of COX-2 in acute pain and the use of selective COX-2 inhibitors for acute pain relief. *Curr Pharm Des* 2005;11:1737–55.
19. Bingham S, Beswick PJ, Blum DE, et al. The role of the cyclooxygenase pathway in nociception and pain. *Semin Cell Dev Biol* 2006;17:544–54.
20. DeLeo TA, Hashizume H, Rutkowski MD, et al. Cyclooxygenase-2 inhibitor SC-236 attenuates mechanical allodynia following nerve root injury in rats. *J Orthop Res* 2000;18:977–82.
21. Kawakami M, Matsumoto T, Hashizume H, et al. Epidural injection of cyclooxygenase-2 inhibitor attenuates pain-related behavior following application of nucleus pulposus to the nerve root in the rat. *J Orthop Res* 2002;20:376–81.
22. Andre S, Boukhaddaoui H, Campo B, et al. Axotomy-induced expression of calcium-activated chloride current in subpopulations of mouse dorsal root ganglion neurons. *J Neurophysiol* 2003;90:3764–73.
23. Li C, Hossieny P, Wu BJ, et al. Pharmacologic induction of heme oxygenase-1. *Antioxid Redox Signal* 2007;9:2227–39.
24. Hirata K, He JW, Kuraoka A, et al. Heme oxygenase1 (HSP-32) is induced in myelin-phagocytosing Schwann cells of injured sciatic nerves in the rat. *Eur J Neurosci* 2000;12:4147–52.
25. Barclay J, Clark AK, Ganju P, et al. Role of the cysteine protease cathepsin S in neuropathic hyperalgesia. *Pain* 2007;130:225–34.
26. Clark AK, Yip PK, Grist J, et al. Inhibition of spinal microglial cathepsin S for the reversal of neuropathic pain. *Proc Natl Acad Sci USA* 2007;104:10655–60.

p63 Induces CD4⁺ T-Cell Chemoattractant TARC/CCL17 in Human Epithelial Cells

Terufumi Kubo, Shingo Ichimiya, Akiko Tonooka, Tsutomu Nagashima, Tomoki Kikuchi, and Noriyuki Sato

To preserve immunosurveillance, epithelial cells support T-cell trafficking toward inflammatory foci. However, how epithelial cells are enrolled in recruiting T cells has not been fully elucidated. In this study we investigated the function of p63, a p53 family member, in the regulation of the expression of various types of chemokine ligands by focusing on the property of p63 as an epitheliotropic transcription factor. As assessed by experiments using three different human epithelial cell lines with small-interfering RNAs or plasmids of p63, certain CC chemokine ligands were found to be under the control of p63. In these CC chemokine ligands, p63 had the common capacity to upregulate TARC/CCL17 in the different cell lines, whose receptor CCR4 was preferentially presented on CD4⁺ T cells such as memory, regulatory, IL-17-producing and type II helper T cells. More interestingly, when cells were stimulated with transforming growth factor- β (TGF- β) or epidermal growth factor (EGF) as observed during tissue repair process, the expression of p63 and TARC/CCL17 was concomitantly suppressed. This implies that, in local inflammatory regions with general epithelial tissue remodeling, the p63-TARC/CCL17 axis may participate in the engagement of efficient immune reactions by specified T-cell subsets.

Introduction

IT IS WELL RECOGNIZED that epithelial cells play an important role in the immune system as the front line of defense against external pathogens (Hayday and others 2001). Anatomically, epithelial cells of tissues such as lung, skin, and intestines tightly connect to each other to form a sheet structure with various junctional molecules (Tsukita and Furuse 2000). These epithelial networks eventually help defend against pathogens and also evoke cellular and molecular interactions of immune responses by recruiting a multitude of inflammatory cells like lymphocytes and dendritic cells (von Andrian and Mackay 2000). In addition to the mechanisms of innate immunity, acquired or adaptive immunity is essential for specific responses to various immunologic insults around epithelial tissues. The mechanism of homing of inflammatory cells to epithelial cells has been extensively investigated and soluble factors, including chemokine ligands, are known to have a pivotal function, but the secretion mechanism by which epithelial cells foster regional lymphocytes is still unclear.

Chemokine ligands are secreted polypeptides that trigger an elaborate process whereby inflammatory cells presenting chemokine receptors of seven-transmembrane G-protein-coupled receptors can promptly channel them to the foci

requiring immune and inflammatory reactions (Kunkel and Butcher 2002; Milligan and Smith 2007). Based on their structural characteristics with regard to the positions of a cysteine residue, chemokine ligands are classified into two major subfamilies: CC and CXC chemokine ligands. To date many different CC and CXC chemokine ligands have been discovered and some of them derived from epithelial tissues are known to play cardinal roles in the emergence of allergic or atopic inflammatory disorders and cancer development (Juremalm and others 2005; Ruffini and others 2007).

Accumulating evidence has indicated that p63, a p53-like molecule, is a usual epithelial constituent and determines properties of epithelial stem cells (Truong and others 2006). Indeed, loss of p63 leads to severe epithelial tissue hypoplasia due to the inhibition of both stratification and differentiation of keratinocytes (Koster and others 2007). Various genes, encoding JAG1, PERP, p21, or 14-3-3 σ , are transactivated by p63, but it is not well investigated whether p63 is involved in the expression of chemokine ligands in epithelial cells (Sasaki and others 2002; Westfall and others 2003; Ihri and others 2005).

In this study we assessed the role of p63 in the regulation of the transcription of a series of chemokine ligands on three different types of human epithelial cells with

small-interfering RNAs (siRNAs) or plasmid DNAs of p63. We clearly found some CC chemokine ligands that could be regulated by p63. Among the chemokine ligands we investigated, the only one that p63 could commonly upregulate in the three epithelial cell lines we investigated was thymus and activation-regulated chemokine (TARC)/CCL17, a strong chemoattractant of CD4⁺ T cells like memory, regulatory and type II Th as well as Th17 cells (Vestergaard and others 2000; Baekkevold and others 2005; Hirahara and others 2006; Lim and others 2008). Tissue remodeling-associated cytokines such as transforming growth factor- β (TGF- β) and epidermal growth factor (EGF) suppressed the expression of p63 of epithelial cells as under the repair process (Kurokawa and others 2006). It was of great interest that, in accordance with the downregulation of p63, cells exposed to these cytokines showed the suppression of TARC/CCL17 as expected. This may illustrate an instructive mechanism mediated by p63, by which epithelial tissues could retain CD4⁺ T-cell populations responsible for immunomodulation ready to be mobilized at the sites of immune reactions during the physiological healing process of epithelial tissues. As TARC/CCL17 is well known to be involved in the emergence of allergic bronchitis and allergic or atopic dermatitis, our observations may lead to further understanding of the mechanisms of such immune-related disorders (Sekiya and others 2000; Campbell and others 2007; Furusyo and others 2007).

Materials and Methods

Cell lines and cell culture

Human LC817, HaCaT, and 293 epithelial cells were maintained in modified Dulbecco's modified Eagle's medium supplemented with 10% heat-inactivated bovine calf serum, 50 μ g/mL streptomycin, and 100 U/mL penicillin. All cells were cultured at 37°C in a humidified atmosphere in 5% CO₂.

Antibodies and immunohistochemistry

The antibody used was a rabbit anti-p63 polyclonal antibody (H-137; Santa Cruz Biotechnology, Santa Cruz, CA, USA). The procedures for immunofluorescence have been previously described (Kikuchi and others 2004). Signals were detected under an immunofluorescence microscope (IX71, Olympus).

RT-PCR and real-time RT-PCR

Primer pairs were selected using Primer3 software on messenger RNA sequences based on the National Center for Biotechnology Information database. Sequences of the primer pairs were finally determined after reference to the original genomic organization presented in the Ensembl database (Sanger Centre), as summarized in Table 1. Real-time polymerase chain reaction (PCR) was performed as described in the manufacturer's protocol for Assays-on-Demand Gene Expression products (Applied Biosystems). To compare the levels of expression of genes, the $\Delta\Delta$ CT method

was employed to analyze triplicate specimens (Livak and Schmittgen 2001).

Transfection of siRNAs and plasmid DNAs

Cells were cultured at a density of 2×10^5 cells/well in a 6-well plate in 2.5-mL culture medium. After 24 h, the culture medium was replaced by medium containing a complex of the siRNAs specific for p63 (B-Bridge) and Lipofectamine RNAi MAX (Invitrogen), giving a final concentration of siRNA of 20 nM following the manufacturer's instructions. After 48 h, cells were harvested to be subjected to real-time PCR analysis. As with transfection of siRNAs, cells were prepared prior to transfection. After 24 h, 250 ng of pcDNA3.1 harboring cDNA encoding p63 (pcDNA3.1-p63) was transiently transfected using Lipofectamine 2000 reagent (Invitrogen). After 48 h, cells were harvested and analyzed.

Cell stimulation

Cells were cultured at a density of 2×10^5 cells 24 h before stimulation. Then the culture medium was replaced by a medium containing 10 U/mL TGF- β (Sigma-Aldrich) or 10 U/mL EGF (Sigma-Aldrich). After 48 h total RNA was harvested from cells to be employed in subsequent real-time PCR analysis.

Results

Chemokine ligands regulated by p63 in LC817 pulmonary epithelial cells

To address the question of whether p63 was involved in the regulation of chemokines of epithelial cells, we initially established a specialized cellular state with suppressed levels of p63 by employing the siRNA technique. When the designated siRNA from a sequence encoding p63 was transiently introduced into LC817 pulmonary epithelial cells that constitutively expressed p63, it was downregulated at transcription and protein levels as well (Fig. 1A). Using these LC817 cells, reverse transcriptase (RT)-PCR analyses of CC chemokine ligands, including CCL1 to CCL28, indicated that the expression of TARC/CCL17, CCL22, CCL25, and CCL28 was likely to be upregulated by p63 (Fig. 1B). CCL5 was also under the control of p63, but was negatively regulated. A series of CXC chemokine ligands was also investigated in LC817 cells, though there were no significant changes of any type of CXC chemokine ligand, including CXC1 to CXC16 at the transcription level (Fig. 1C). Thus p63 could regulate the levels of CC chemokine ligands of CCL5, TARC/CCL17, CCL22, CCL25, and CCL28 but not CXC chemokine ligands in LC817 cells.

Chemokine ligands regulated by p63 in HaCaT epidermal cells

To evaluate the results obtained from the analysis of LC817 cells, we further examined HaCaT epidermal cells, which also endogenously expressed p63. Prior to RT-PCR analyses, it was also confirmed that HaCaT cells with the siRNAs of p63

TABLE 1. PRIMER SEQUENCES USED IN THIS STUDY.

Gene name	Length (bp)	(Forward primer)			(Reverse primer)		
		sequence (5'-3')	Temp(°C)	Position	sequence (5'-3')	Temp(°C)	Position
CCL1	163	catttgccggagcaagagatt	60.4	exon2	tgccctcagcatttttctgtg	60.0	exon3
CCL2	171	ccccagtcacctgctgttat	60.0	exon2	tggaatcctgaaccacttc	59.9	exon3
CCL3	198	tgcaaccagttctctgcatc	60.0	exon1	tttctggaccactcctcac	60.1	exon3
CCL4	211	aagctctgctgactgtcct	60.2	exon1	gcttgcttcttttggttgg	59.9	exon3
CCL5	150	cgctgtcatcctcattgcta	60.0	exon1	gagcacttgccactggtgta	59.9	exon2
CCL7	179	atgaaagcctctgcagcact	60.2	exon1	ggacagtggctactggtggt	60.0	exon2
CCL8	192	aatgtccaaggaagctgtg	60.1	exon2	gggagggtgggaaaataaa	60.0	exon3
CCL11	233	agaaaccaccactctcacg	60.2	exon1	cacagcttctggggacatt	60.1	exon2
CCL13	245	atctccttgacagaggctgaa	60.1	exon2	agaagaggagccagaggag	60.1	exon3
CCL14/15	214	tcccgtgtcactcatgaaa	60.1	exon3	tcagaggctcaggagggtt	60.0	exon4-5
CCL16	242	ctgccctgtctctctgtc	60.0	exon1	ctcttgaccactgctcat	60.1	exon3
CCL17	163	ctfctctgcagcacatccac	59.6	exon1	ctgccctgcacagttaaaa	59.9	exon3
CCL18	150	agctctgctgcctctgtat	59.4	exon2	cccacttctattggggta	59.8	exon3
CCL19	172	atccctgggtacatctgag	59.8	exon2	gcttcatcttggtgagtc	60.0	exon3
CCL20	198	ttattgtgggcttcacacg	59.6	exon2	tgggctatgtccaattccat	60.2	exon3
CCL21	220	caagcttaggctgctccatc	60.1	exon2	tcagtctcttgagccttt	60.1	exon3
CCL22	212	cgctgtgtaaacacttcta	59.9	exon2	ataatggcaggaggtaggg	60.2	exon3
CCL23	173	tttgaacgaacagcgagt	60.0	exon3	tgtgtccctcaccttgaca	60.1	exon4
CCL24	228	gccttctgtctctgtgtc	59.7	exon1	tgtaccttgaccactcc	60.0	exon3
CCL25	198	acaggaagggtgtggtgaa	59.9	exon3	tactgctgctgatgggattg	59.8	exon4
CCL26	163	ggaggagtttgggagaaac	59.9	exon2	tgtggctgtattggaagcag	59.9	exon3
CCL27	191	agcactgctgctgtactca	59.8	exon2	tcttggtgctcaaccactg	59.9	exon3
CCL28	188	gctgatggggattgtgactt	59.9	exon2	ccctgatgtgccctgttact	60.0	exon3
CXCL1	171	agggaattcacccaagaac	60.2	exon2	tggattgtcactgttcagca	60.3	exon2-3
CXCL2	172	gcaggaattcacctcaaga	60.2	exon2	ggatttgcatttttcagc	61.0	exon3-4
CXCL3	172	gcaggaattcacctcaaga	60.2	exon2	gggtctcccctgttctcag	61.0	exon3-4
CXCL4	174	gctgctctgccactgt	60.2	exon1	ttcagcgtgctatcagttg	60.0	exon2-3
CXCL5	171	gcaaggagtcatcccaaaa	60.1	exon2	ttgtttccaccgtccaaaat	60.2	exon3-4
CXCL6	158	gtctgtctctgctgtctg	59.8	exon2	aacttgctcccgcttcttca	59.9	exon3
CXCL7	207	tcctccacaaaggacaaac	59.9	exon1	ttctccactcctcagtg	60.0	exon3
CXCL8	196	gtgcagttttccaaggagt	60.3	exon1-2	ctctgcaccagtttctct	59.3	exon4
CXCL9	166	tttctcttgggcatcatc	60.0	exon1	tcaatttctgcaggaagg	60.3	exon2
CXCL10	172	ctgtacgctgtacctgcatca	59.9	exon2	ttctgtatggccttcgattc	60.2	exon3
CXCL11	175	agaggacgctgtcttgcac	60.0	exon2	taagcctgtctgcttcgat	60.1	exon3
CXCL12	161	tcagcctgagctacagatgc	59.3	exon2	cttagcttcgggtcaatgc	59.9	exon3
CXCL13	151	gcttgagggttagatgtgtcca	60.2	exon2	tgagggtccacacacaaat	59.9	exon3
CXCL14	152	aagctggaatgaagccaaa	59.8	exon2	ttccaggcgttgtaccactt	60.6	exon3
CXCL16	160	tctccggaacacctgagag	60.4	exon2	cacaatccccgagtaagcat	60.0	exon4
p63	163	gaaacgtacaggcaacagca	59.9	exon10	gctgctgagggttgataagc	60.0	exon11

expressed p63 to a lesser extent than control cells (Fig. 2A). As assessed by RT-PCR analyses, CCL7, TARC/CCL17, and CCL26 were upregulated by p63 in HaCaT cells (Fig. 2B). In HaCaT cells, CCL5 was also slightly upregulated and CCL25 was downregulated by p63, though p63 insignificantly affected the expression of CCL22 and CCL28. These results, except for TARC/CCL17, did not match those of LC817 cells, suggesting that the manner of p63 regulation of CC chemokine ligands probably varied by epithelial cell type. Thus TARC/CCL17 was thought to be a particular CC chemokine ligand with a mechanism of transcription regulated by p63 that might be common in usual epithelial cells.

Excess amounts of p63 induce TARC/CCL17 in 293 epithelial cells

Following these results, we next employed an alternative approach to determine whether CC chemokine ligands CCL5, CCL7, TARC/CCL17, CCL22, CCL25, CCL26, and CCL28 were regulated by p63. As 293 epithelial cells did not endogenously express p63, the cells were transiently transfected with p63 plasmids. Interestingly RT-PCR analyses of 293 cells with excess p63 demonstrated high amounts of TARC/CCL17 (Fig. 3). The levels of CCL5 and CCL26 were relatively decreased in 293 cells with excess p63. This was

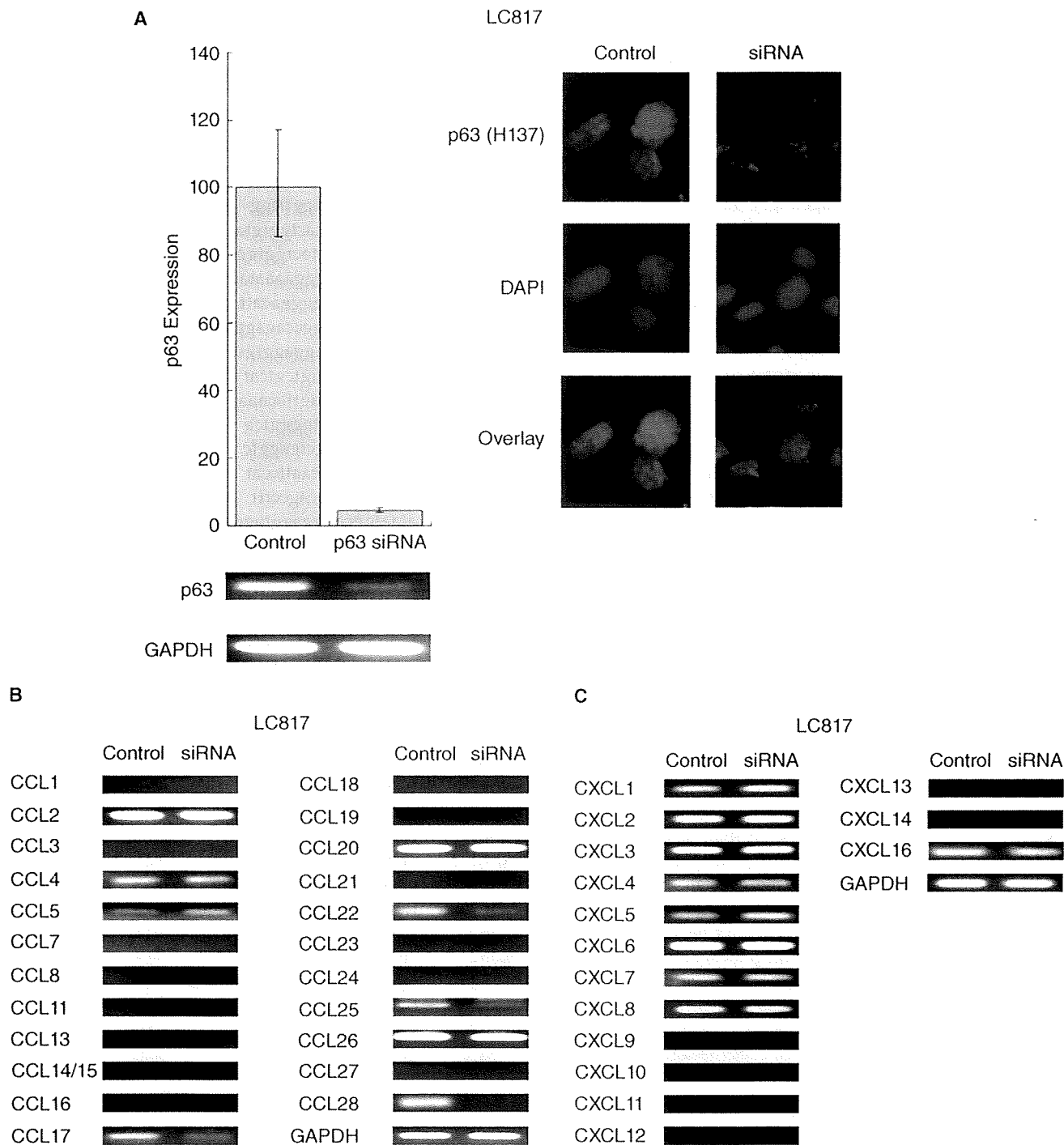


FIG. 1. Transcription analysis of LC817 pulmonary epithelial cells. **(A)** Transfection of siRNAs specific for p63 resulted in the downregulation of p63 in LC817 cells. Left panels show real-time PCR analysis of cDNAs derived from cells with siRNA specific for GFP or siRNA specific for p63. Simultaneously, cDNAs were checked by RT-PCR analysis of p63. Right panels show immunofluorescence analysis of cells with siRNA of GFP or p63 (depicted as control and siRNA, respectively), where p63 is visualized by H137 pAb in red and the nucleus by DAPI in blue. **(B and C)** Transcription profiles as assessed by RT-PCR analysis of CC and CXC chemokine ligands, respectively. Control, cells transfected with GFP siRNAs; p63 siRNA or siRNA, cells with p63 siRNAs; GAPDH, a template control.

similarly found in LC817 and HaCaT cells, suggesting that p63 was probably associated with the control of the expression of CCL5 through various factors depending on the

cells. In 293 cells, the levels of CCL22, CCL25, and CCL28 were not altered and CCL7 seemed not to be associated with p63. Collectively, the mechanism by which p63 positively

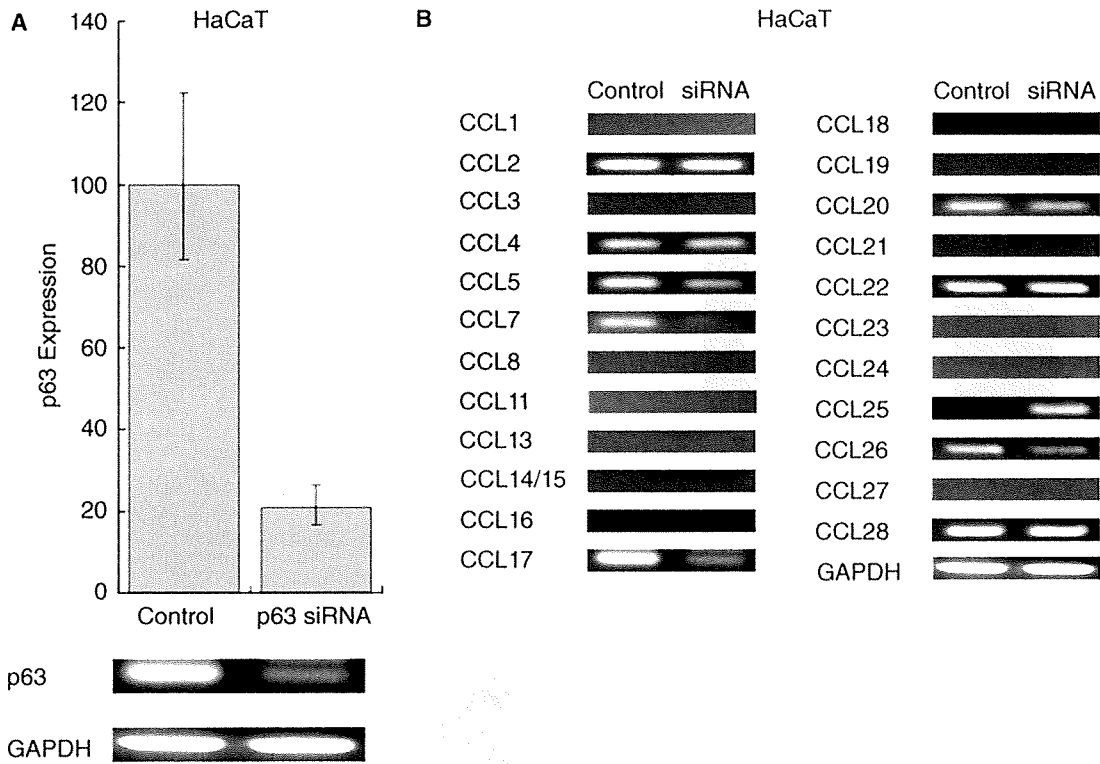


FIG. 2. Transcription analysis of HaCaT epidermal cells. (A) Transfection of siRNAs specific for p63 resulted in the down-regulation of p63 in HaCaT cells. Real-time PCR analysis of cDNAs derived from cells with siRNA specific for GFP and with siRNA specific for p63. Simultaneously, cDNAs were evaluated by RT-PCR analysis of p63 and GAPDH as a template control. (B) Transcription profiles as assessed by RT-PCR analysis of CC chemokine ligands in HaCaT cells. Control, cells transfected with GFP siRNAs; siRNA, cells transfected with p63 siRNAs; GAPDH, a template control.

induced the expression of TARC/CCL17 would generally appear to be shared by human epithelial cells. It was also observed that CCL5 and CCL26 were under the control of p63 in specific types of epithelial cells.

TGF-β and EGF downregulate p63 and TARC/CCL17

It is well recognized that inflammatory responses are usually accompanied by inflammatory healing reactions around local epithelial tissues. A complex mechanism with multiple inflammatory cells underlays these reactions, in which TGF-β and EGF have pivotal roles in such remodeling during immune responses. When epithelial remodeling around inflammatory foci occurs, the levels of p63 are mostly suppressed in epithelial cells (Bamberger and others 2005; Kurokawa and others 2006). To examine the physiological role of p63 in the context of TARC/CCL17 expression, HaCaT cells were stimulated with TGF-β or EGF. As under inflammatory conditions, the levels of p63 were inhibited in these cells down to ~40–50% of the control levels (Fig. 4). As expected due to the downregulation of p63, the levels of TARC/CCL17 were significantly decreased to 5–10% of the control levels. This may imply physiological association of TGF-β and EGF with the regulation of TARC/CCL17 through p63.

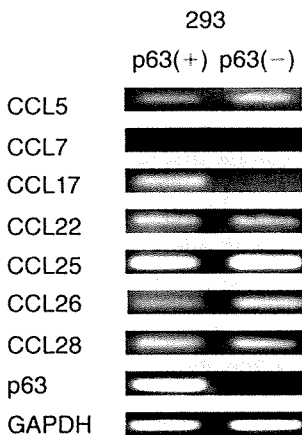


FIG. 3. Transcription analysis of CCL5, CCL7, CCL17, CCL22, CCL25, CCL26, and CCL28 in 293 epithelial cells with transiently introduced mock pcDNA3.1 or p63-pcDNA3.1 (depicted as p63(-) or p63(+), respectively) by RT-PCR. GAPDH, a template control.

Discussion

In this study, we first identified a role of the p63 molecule in the positive regulation of TARC/CCL17 in human

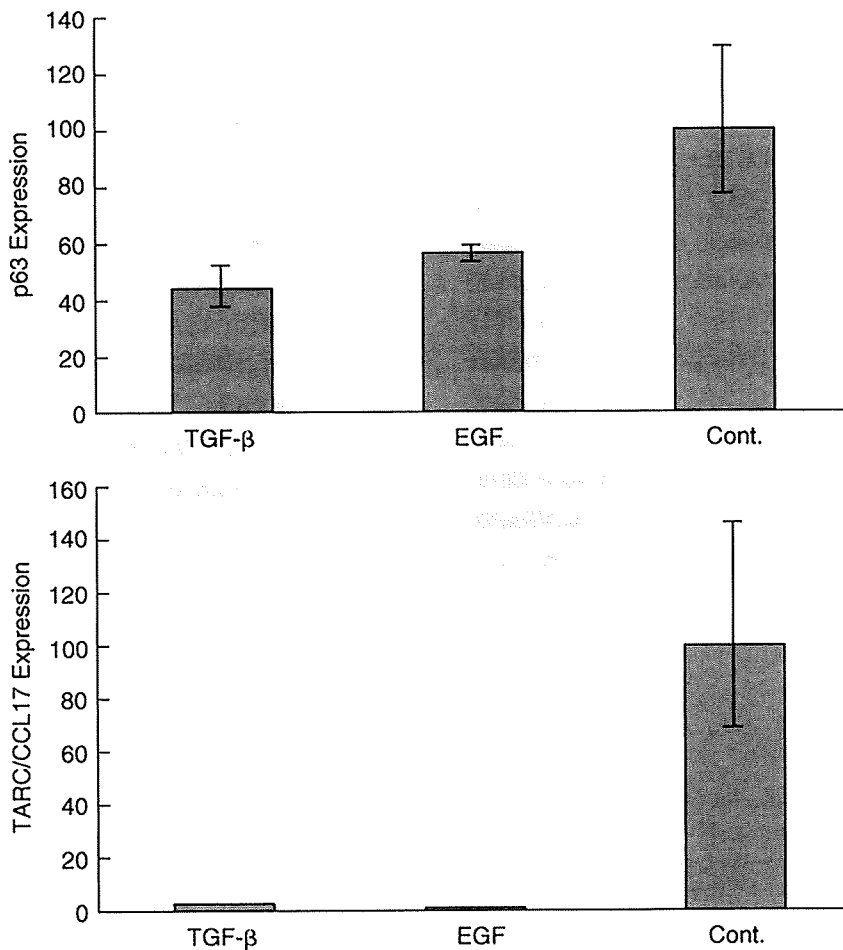


FIG. 4. Transcription analysis of p63 and TARC/CCL17 in HaCaT cells stimulated with TGF- β or EGF associated with tissue remodeling by real-time PCR. *Upper and lower panels* show levels of transcription of p63 and TARC/CCL17, respectively.

epithelial cells. The transcripts of TARC/CCL17 are exclusively detected in epithelial tissues, including lung and small and large intestines as well as thymus, suggesting that TARC/CCL17 mainly acts as a chemokine of epithelial origin (Imai and others 1996). Because p63 shows an expression profile with TARC/CCL17 in various human epithelial tissues, our results are compatible with the functional correlations implied by the expression profiles of p63 and TARC/CCL17 (Schmale and Bamberger 1997; Kikuchi and others 2004). Similar to the adhesion molecules, chemokines and their surface receptors can be up- or downregulated as cells undergo differentiation or stimulation, allowing lymphocytes to coordinate their own pathway with their immunologic functions. In this context, it is intriguing that TGF- β and EGF suppressed the levels of TARC/CCL17, probably through downregulation of p63, as during the inflammatory healing process, where external pathogens can enter into the tissues from the openings of broken epithelial cell sheets. This might imply that the p63-TARC/CCL17 axis participates in the homing and release of particular T-cell subsets and then engages efficient immune reactions at local inflammatory regions with epithelial tissue remodeling.

Since CD4⁺ T cells chiefly conduct immunosurveillance, they have to be mobilized to the sites where antigens are

localized and presented through a major histocompatibility complex or CD1 (Bendelac and others 2007). TARC/CCL17 specifically binds to the CC chemokine receptor CCR4 on the surface of the CD4⁺ T cell. It is noteworthy that memory and regulatory T cells, Th17 and Th2 CD4⁺ T cells, possess CCR4 and are possibly able to home through TARC/CCL17 in skin, lung, and tumor tissues (Vestergaard and others 2000; Backkevoold and others 2005; Hirahara and others 2006; Lim and others 2008). Active involvement of TARC/CCL17 has also been reported in the emergence of allergic as well as atopic disorders in skin and lung (Sekiya and others 2000; Campbell and others 2007; Furusyo and others 2007). According to the Th1/Th2 paradigm, inflammation associated with allergic disorders is regarded as a Th2-dominant immune response. The cytokines liberated by allergen-reactive Th2 cells control the process leading to allergic inflammation. Thus specific control of p63 expression may lead to a new modality for the control of allergic and atopic disorders, or even cancer, through alteration of the levels of TARC/CCL17 (Ishida and Ueda 2006; Saeki and Tamaki 2006).

Previously we have reported that p63 can also activate the gene expression of human inter-cellular adhesion molecule 1 (ICAM-1), which plays a role in the binding of T cells through lymphocyte function-associated antigen-1 (LFA-1)

to epithelial cells. This mechanism may further work to enforce the affinity of epithelial cells to T cells. The promoter region of the ICAM-1 gene responsive to p63 is restricted, with a 135-bp region where an interferon- γ -activated sequence (GAS) motif, Sp-1, and AP-2 are localized (Kikuchi and others 2004). It is noteworthy that this GAS motif is seemingly shared by the proximal promoter sequence of TARC/CCL17 (Maier and others 2007). However, within a promoter sequence from 950-bp to the transcription start site of the TARC/CCL17 promoter region, we failed to find a sequence that completely matched the specific motif directly bound to p63 reported recently (Perez and others 2007). Thus it is possible to consider that p63 indirectly modulates the transactivation of the TARC/CCL17 gene through GAS or other motifs via an as yet unidentified mechanism, although more experiments will be required to determine the precise action of p63 in the regulation of these genes.

In summary, we reported novel involvement of p63 in the regulation of TARC/CCL17 of epithelial tissues under tissue repair. To respond rapidly and effectively to various immunologic insults, the coordinated action of various resident cell populations around epithelial cells as well as immigrating leukocytes enables the mucosal immune system. Our results may also shed light on the role of p63 in epithelial immune surveillance in terms of maintaining peripheral T-cell tolerance as well (Sather and others 2007).

Acknowledgments

This work was in part supported by grants-in-aid for Scientific Research (C) from JSPS (No. 20590347) and from the Akiyama Foundation to S. Ichimiya.

References

- Baekkevold ES, Wurbel MA, Kivisäkk P, Wain CM, Power CA, Haraldsen G, Campbell JJ. 2005. A role for CCR4 in development of mature circulating cutaneous T helper memory cell populations. *J Exp Med* 201:1045–1051.
- Bamberger C, Hafner A, Schmale H, Werner S. 2005. Expression of different p63 variants in healing skin wounds suggests a role of p63 in reepithelialization and muscle repair. *Wound Repair Regen* 13:41–50.
- Bendelac A, Savage PB, Teyton L. 2007. The biology of NKT cells. *Annu Rev Immunol* 25:297–336.
- Campbell JJ, O'Connell DJ, Wurbel MA. 2007. Cutting edge: chemokine receptor CCR4 is necessary for antigen-driven cutaneous accumulation of CD4 T cells under physiological conditions. *J Immunol* 178:3358–3362.
- Furusyo N, Takeoka H, Toyoda K, Murata M, Maeda S, Ohnishi H, Fukiwake N, Uchi H, Furue M, Hayashi J. 2007. Thymus and activation regulated chemokines in children with atopic dermatitis: Kyushu University Ishigaki Atopic Dermatitis Study (KIDS). *Eur J Dermatol* 17:397–404.
- Hayday A, Theodoridis E, Ramsburg E, Shires J. 2001. Intraepithelial lymphocytes: exploring the Third Way in immunology. *Nat Immunol* 2:997–1003.
- Hirahara K, Liu L, Clark RA, Yamanaka K, Fuhlbrigge RC, Kupper TS. 2006. The majority of human peripheral blood CD4⁺CD25^{high}Foxp3⁺ regulatory T cells bear functional skin-homing receptors. *J Immunol* 177:4488–4494.
- Ihrig RA, Marques MR, Nguyen BT, Horner JS, Papazoglu C, Bronson RT, Mills AA, Attardi LD. 2005. Perp is a p63-regulated gene essential for epithelial integrity. *Cell* 120:843–856.
- Imai T, Yoshida T, Baba M, Nishimura M, Kakizaki M, Yoshie O. 1996. Molecular cloning of a novel T cell-directed CC chemokine expressed in thymus by signal sequence trap using Epstein-Barr virus vector. *J Biol Chem* 271:21514–21521.
- Ishida T, Ueda R. 2006. CCR4 as a novel molecular target for immunotherapy of cancer. *Cancer Sci* 97:1139–1146.
- Juremalm M, Olsson N, Nilsson G. 2005. CCL17 and CCL22 attenuate CCL5-induced mast cell migration. *Clin Exp Allergy* 35:708–712.
- Kikuchi T, Ichimiya S, Kojima T, Crisa L, Koshiba S, Tonooka A, Kondo N, Van Der Saag PT, Yokoyama S, Sato N. 2004. Expression profiles and functional implications of p53-like transcription factors in thymic epithelial cell subtypes. *Int Immunol* 16:831–841.
- Koster MI, Dai D, Marinari B, Sano Y, Costanzo A, Karin M, Roop DR. 2007. p63 induces key target genes required for epidermal morphogenesis. *Proc Natl Acad Sci USA* 104:3255–3260.
- Kunkel EJ, Butcher EC. 2002. Chemokines and the tissue-specific migration of lymphocytes. *Immunity* 16:1–4.
- Kurokawa I, Mizutani H, Kusumoto K, Nishijima S, Tsujita-Kyutoku M, Shikata N, Tsubura A. 2006. Cytokeratin, filaggrin, and p63 expression in reepithelialization during human cutaneous wound healing. *Wound Repair Regen* 14:38–45.
- Lim HW, Lee J, Hillsamer P, Kim CH. 2008. Human Th17 cells share major trafficking receptors with both polarized effector T cells and FOXP3⁺ regulatory T cells. *J Immunol* 180:122–129.
- Livak KJ, Schmittgen TD. 2001. Analysis of relative gene expression data using real-time quantitative PCR and the $2^{-\Delta\Delta C(T)}$ method. *Methods* 25:402–408.
- Maier E, Wirnsberger G, Horejs-Hoeck J, Duschl A, Hebenstreit D. 2007. Identification of a distal tandem STAT6 element within the CCL17 locus. *Hum Immunol* 68:986–992.
- Milligan G, Smith NJ. 2007. Allosteric modulation of heterodimeric G-protein-coupled receptors. *Trends Pharmacol Sci* 28:615–620.
- Perez CA, Ott J, Mays DJ, Pietenpol JA. 2007. p63 consensus DNA-binding site: identification, analysis and application into a p63MH algorithm. *Oncogene* 26:7363–7370.
- Ruffini PA, Morandi P, Cabioglu N, Altundag K, Cristofanilli M. 2007. Manipulating the chemokine-chemokine receptor network to treat cancer. *Cancer* 15:109:2392–2404.
- Saeki H, Tamaki K. 2006. Thymus and activation regulated chemokine (TARC)/CCL17 and skin diseases. *J Dermatol Sci* 43:75–84.
- Sasaki Y, Ishida S, Morimoto I, Yamashita T, Kojima T, Kihara C, Tanaka T, Imai K, Nakamura Y, Tokino T. 2002. The p53 family member genes are involved in the Notch signal pathway. *J Biol Chem* 277:719–724.
- Sather BD, Treuting P, Perdue N, Miazgowiec M, Fontenot JD, Rudensky AY, Campbell DJ. 2007. Altering the distribution of Foxp3⁺ regulatory T cells results in tissue-specific inflammatory disease. *J Exp Med* 204:1335–1347.
- Schmale H, Bamberger C. 1997. A novel protein with strong homology to the tumor suppressor p53. *Oncogene* 15:1363–1367.
- Sekiya T, Miyamasu M, Imanishi M, Yamada H, Nakajima T, Yamaguchi M, Fujisawa T, Pawankar R, Sano Y, Ohta K, Ishii A, Morita Y, Yamamoto K, Matsushima K, Yoshie O, Hirai K. 2000. Inducible expression of a Th2-type CC chemokine thymus- and activation-regulated chemokine by human bronchial epithelial cells. *J Immunol* 165:2205–2213.
- Truong AB, Kretz M, Ridky TW, Kimmel R, Khavari PA. 2006. p63 regulates proliferation and differentiation of developmentally mature keratinocytes. *Genes Dev* 20:3185–3197.

- Tsukita S, Furuse M. 2000. The structure and function of claudins, cell adhesion molecules at tight junctions. *Ann NY Acad Sci* 915:129–135.
- Vestergaard C, Bang K, Gesser B, Yoneyama H, Matsushima K, Larsen CG. 2000. A Th2 chemokine, TARC, produced by keratinocytes may recruit CLA+CCR4+ lymphocytes into lesional atopic dermatitis skin. *J Invest Dermatol* 115:640–646.
- von Andrian UH, Mackay CR. 2000. T cell function and migration. Two sides of the same coin. *N Engl J Med* 343:1020–1034.
- Westfall MD, Mays DJ, Sniezek JC, Pietenpol JA. 2003. The Δ Np63 phosphoprotein binds the p21 and 14–3–3s promoters in vivo and has transcriptional repressor activity that is reduced by Hay-Wells syndrome-derived mutations. *Mol Cell Biol* 23:2264–2276.

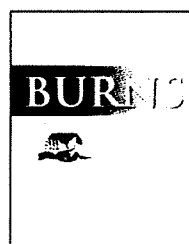
Address reprint requests or correspondence to:
Shingo Ichimiya, M.D., Ph.D.
Department of Pathology
Sapporo Medical University School of Medicine
Sapporo 060-8557
Japan

Tel: +81-11-611-2111 (ext. 2691)

Fax: +81-11-643-2310

E-mail: ichimiya@sapmed.ac.jp

Received 24 March 2008/Accepted 31 May 2008



Immunosuppressive effect on T cell activation by interleukin-16- and interleukin-10-cDNA-double-transfected human squamous cell line

Yoshitaka Matsumoto^{a,*}, Tatsuya Fujita^a, Itaru Hirai^b, Hiroeki Sahara^b, Toshihiko Torigoe^b, Kyori Ezo^a, Tamotsu Saito^a, William W. Cruikshank^c, Takatoshi Yotsuyanagi^a, Noriyuki Sato^b

^a Division of Plastic Surgery, Sapporo Medical University School of Medicine, South-1, West-16, Chuo-ku, Sapporo 060-8543, Japan

^b Department of Pathology, Sapporo Medical University School of Medicine, South-1, West-16, Chuo-ku, Sapporo 060-8543, Japan

^c Pulmonary Center, Boston University School of Medicine, Boston, MA, USA

ARTICLE INFO

Article history:

Accepted 30 June 2008

Keywords:

Allogeneic skin graft
Interleukin-16
Interleukin-10
Gene therapy
Artificial skin

ABSTRACT

It is well known that induction of immunotolerance with allogeneic skin transplantation is generally difficult. This study attempted to find an immunosuppressive protocol for skin allograft rejection involving interleukin-16 (IL-16) and interleukin-10 (IL-10), because both are known to inhibit mixed lymphocyte reaction (MLR). The data indicated that IL-16 enhanced the immunosuppressive effect of IL-10. IL-16-cDNA- and IL-10-cDNA-double-transfected squamous cell carcinoma cell line were used as an *in vitro* model and they produced more than 20 ng/ml of IL-16 and 100 pg/ml of IL-10 in the supernatant, which significantly inhibited MLR and also the activation of allogeneic lymphocytes, which were stimulated directly by allogeneic double-cDNA-transfectant cells. Thus allogeneic skin graft producing IL-16 and IL-10 might have a local immunosuppressive action that could prolong graft survival.

© 2008 Elsevier Ltd and ISBI. All rights reserved.

1. Introduction

The transplantation of skin allograft has long been used to treat extensive burns; its biological effects on re-epithelialisation and neovascularisation have been investigated [1–3]. Skin allograft functions as a temporary barrier to bacterial invasion and also water and protein loss, compensating for skin function and improving the general condition of the burn victim. However, skin allograft rejection usually occurs 2–3 weeks after transplantation. Thus it is important to seek how to prolong skin allograft survival.

Previously, we confirmed that interleukin-16 (IL-16), which is considered one of the natural ligands of the CD4 molecule,

enhanced an immunosuppressive effect of anti-CD4 monoclonal antibody (mAb). Furthermore, IL-16-cDNA-transfected keratinocyte-equivalent squamous cells directly inhibited allogeneic lymphocyte activation [4]. In this study, we evaluated the effect of another inhibitory cytokine, interleukin-10 (IL-10), which is known to inhibit mixed lymphocyte reaction (MLR) in the T cell response [5]. Our present data suggested that IL-10 in conjunction with IL-16 inhibited MLR more efficiently than either cytokine alone. This implies that allogeneic skin cells producing IL-16 and IL-10 might induce local immunosuppression or local tolerance, and consequently prolong allogeneic skin graft survival. We aimed to show whether IL-16-cDNA- and IL-10-cDNA-double-trans-

* Corresponding author. Tel.: +81 11 611 2111; fax: +81 11 615 0916.

E-mail address: ymatsu@sapmed.ac.jp (Y. Matsumoto).

0305-4179/\$36.00 © 2008 Elsevier Ltd and ISBI. All rights reserved.

doi:10.1016/j.burns.2008.06.017

ected keratinocyte-equivalent squamous cells inhibited allogeneic lymphocyte activation more efficiently, which suggests the possible development of an immunoregulatory skin allograft.

2. Materials and methods

2.1. Recombinant human IL-16 and IL-10

The preparation of recombinant human IL-16 (rIL-16) was described previously [4]. Briefly, to construct the *Escherichia coli* expression vector for His-tagged human IL-16, human IL-16-cDNA was amplified by polymerase chain reaction (PCR) and ligated into pET-16b *E. coli* expression vector (Novagen, Madison, WI, USA). The construct was transformed into *E. coli* BL21 (DE3); bacterial transformant was grown at 37 °C, and His-tagged rIL-16 was induced with 1 mM of isopropyl β -D-thiogalactopyranoside at 37 °C for 2 h. The recombinant protein was purified by His TrapTM (Pharmacia Biotech, Uppsala, Sweden) following the manufacturer's protocol. Recombinant human IL-10 (rIL-10) was purified by the same procedure.

2.2. Immunosuppressive effect of rIL-16 and rIL-10 on MLR

Human peripheral blood lymphocytes (PBL) from healthy human volunteers were obtained by density centrifugation and washed with phosphate-buffered saline (PBS). Stimulator cells were prepared by incubating cells at 10^6 ml^{-1} with 25 $\mu\text{g/ml}$ mitomycin C for 20 min. After four washes with PBS, they were suspended with RPMI1640 (Nissui, Tokyo, Japan) supplemented with 25 mM HEPES buffer, 100 U/ml penicillin, 100 $\mu\text{g/ml}$ streptomycin and 10% fetal calf serum (FCS; Filtron, Brooklyn, Australia) (complete medium) at 10^6 ml^{-1} . Responder PBL were supplemented in complete medium and incubated in a nylon wool column (Iwaki, Tokyo, Japan) for 60 min at 37 °C in 5% CO_2 . The nylon wool non-adherent T cells, which were >97% T lymphocytes as determined by staining with anti-CD3 mAb (Becton-Dickinson, Franklin Lakes, NJ, USA), were then suspended in complete medium at 10^6 ml^{-1} and preincubated with 10^{-8} M of rIL-16 or bovine serum albumin (BSA) alone and, in some experiments, with 0.01 $\mu\text{g/ml}$ of rIL-10, at 37 °C in 5% CO_2 for 1 h before the addition of stimulator cells. BSA, 10 $\mu\text{g/ml}$, was used as an irrelevant control protein. We confirmed that 10 $\mu\text{g/ml}$ of BSA did not affect the MLR because there was no significant difference in the MLR with or without BSA (data not shown). Responder and stimulator cells were mixed in a 1:1 ratio and aliquoted into triplicate wells of 96-well round-bottom plates. The cells were cultured at 37 °C in 5% CO_2 , pulsed with [³H]-thymidine on day 4 after the cultivation, and harvested with a SKATRON harvester (Markham, ON, Canada). The radioactivity was counted in a LS6000 scintillation counter on day 5.

2.3. Squamous cell culture, plasmid construction and transfection

The human oral squamous cell carcinoma cell line OSC-20 (HLA-A2, A11, B46, B55, Cw1, Cw9, DR5, DR8, DQ1, DQ7) was

established in our laboratory [6]. Its appearance is epithelial in shape, it grows in a cobblestone pattern with scattered tonofilaments and desmosomes in the intercellular connection, and is positive for cytokeratins and vimentin [7]. It was cultured in RPMI1640 (Nissui, Tokyo, Japan) supplemented with 10% (v/v) FCS. We previously made the human IL-16-cDNA-transfected OSC-20 cell clone, OSC-20-IL16#4, which secreted 50 ng/ml of IL-16 as well as control plasmid (pcDSR α -E3 without IL-16-cDNA)-transfected OSC-20 cells, OSC-20-pcDSR α [4]. These were maintained in selective medium containing puromycin (1 $\mu\text{g/ml}$; Gibco BRL, NY, USA). Before DNA transfection, the cell monolayers were washed twice with PBS and detached by the treatment with 0.05% (w/v) trypsin with 0.02% (w/v) ethylene diamine tetraacetic acid (EDTA; Gibco BRL, NY, USA) in PBS. Cells were then washed with RPMI1640 containing 10% FCS.

Human IL-10-cDNA was constructed into the retrovirus expression vector pLXSN (Clontech, CA, USA). This construct was designated pLXSN-hIL-10. Approximately 10^6 cells of OSC-20-IL16#4 and OSC-20-pcDSR α were transfected with 10 μg of pLXSN-hIL-10 and control plasmids pLXSN without IL-10-cDNA, using the LipofECTAMINE 2000 transfection reagent (Gibco BRL, NY, USA) following the manufacturer's protocol. The transfection mixture was replaced with a fresh medium, and after 48 h it was replaced again with a selective medium containing 1 $\mu\text{g/ml}$ puromycin (Gibco BRL, NY, USA) and 500 $\mu\text{g/ml}$ geneticin (Sigma, St. Louis, MO, USA). Half the medium was changed every 3 days and cells were grown for 3 weeks. Puromycin- and geneticin-resistant cells were transferred into a 96-well dish at a single cell per well, and the clones were obtained and maintained in the selective medium.

Quantitative determination of IL-10 production in these transfectants was performed by colorimetric enzyme-linked immunosorbent assay (ELISA), Cytoscreen hIL-10 (BioSource International, Camarillo, CA, USA) following the manufacturer's protocol. The supernatants of culture medium were collected 24 h after the cultivation of approximately 10^6 cells in culture flasks (Falcon #3024, Franklin Lakes, NJ, USA). Samples (100 μl) of the supernatant were added to ELISA plates to measure IL-10 content in the supernatant, following treatment with the blocking buffer. Colorimetric change was measured at 450 nm by a spectrophotometer and compared with a standard curve of rIL-10. To examine the biological activity of secreted IL-16 and IL-10, supernatants of the cells were added to the MLR experiment. The control comprised OSC-20 cells transfected with the vectors pcDSR α -E3, pBabe Puro [8] and pLXSN. In order to determine the additive effect of secreted IL-16 and IL-10, we used anti-IL-10 mAb (IgG1), kindly gifted by Dr. Ishida of Kyoto University School of Medicine, Kyoto, Japan, and anti-rat natural killer target molecule mAb 109 (IgG1) [9] as isotype-matched control mAb.

2.4. Direct MLR between IL-16- and IL-10-cDNA-double-transfected OSC-20 lines and T cells

The responder T cells were mixed at a 10:1 ratio with the stimulator cells: IL-16- and IL-10-cDNA-double-transfected OSC-20 clones, etc. The ratio when the responder T cells most proliferated in response to the control stimulatory squamous

cells was 10:1 (data not shown). Therefore we tested the ability of transfected squamous cells to suppress T cell responses at this ratio. Stimulator cells were irradiated with 6000 rad in advance. These mixtures were aliquoted into triplicate wells of a 96-well round-bottom plate. The cells were cultured at 37 °C in 5% CO₂, pulsed with [³H]-thymidine on day 4, and harvested with a SKATRON harvester. The radioactivity was counted in a LS6000 scintillation counter on day 5.

In order to determine the level of expression of major histocompatibility complex (MHC) class I and class II molecules in these transfectant cells, we used W6/32 mAb [10] and L243 mAb [11], respectively. W6/32 mAb reacts with MHC class I molecules and L243 mAb reacts with human leukocyte antigen-DR (HLA-DR).

2.5. Statistical analysis

Student's t-test was used to assess the differences between data sets.

3. Results

3.1. The additive effect of human rIL-16 and rIL-10 on human MLR

We recently reported that IL-16-producing allogeneic skin graft might have a local immunosuppressive action that would prolong graft survival [4]. Following this line of study, in order to achieve this local immunosuppressive action more efficiently, we attempted to use IL-16 together with another well-known immunosuppressive cytokine, IL-10 [12], determining the immunosuppressive action of human IL-16 with or without human IL-10. To this end, we obtained recombinant human IL-16 and recombinant human IL-10, and their effects on human MLR were assessed using allogeneic lymphocytes of healthy volunteers. The HLA-haplotypes of responder and stimulator lymphocytes involved were HLA-A2, A33, B17, B61, Cw3, DR6, and HLA-A24, B52, B61, Cw3, DR2, DR8, respectively. As shown in Fig. 1, MLR was inhibited by the

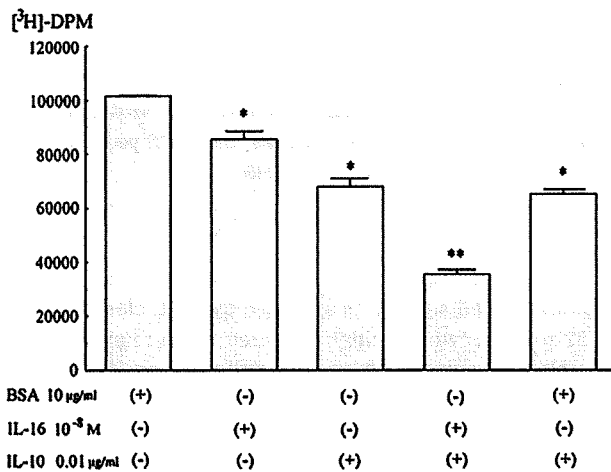


Fig. 1 – Additive action of rIL-16 and rIL-10 on MLR proliferation. Bars represent ±standard error. *p < 0.05 and **p < 0.01.

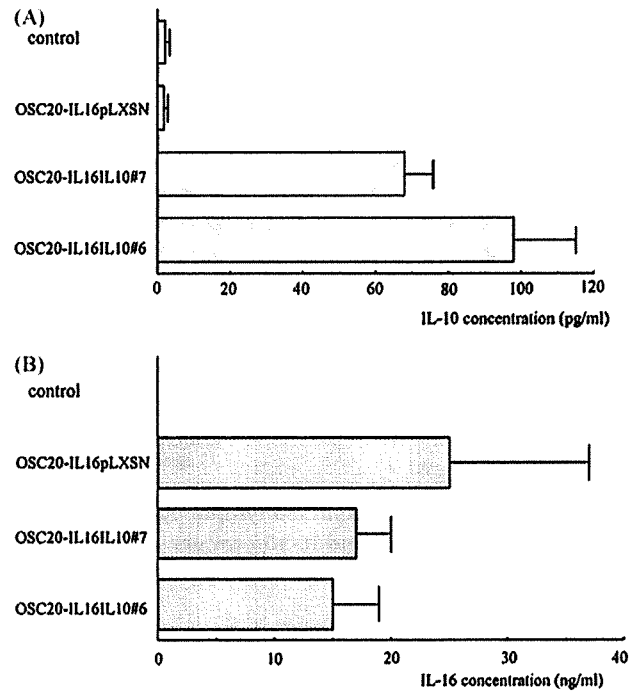


Fig. 2 – (A) IL-10 and (B) IL-16 production in the supernatant of the puromycin-geneticin-resistant squamous cell line OSC-20 clones IL16IL10#6 and #7. Bars represent ±standard error.

addition of 10⁻⁸ M rIL-16 alone or 0.01 µg/ml of rIL-10 alone; this inhibition was clearly enhanced when IL-10 and IL-16 were used together, whereas control protein BSA did not inhibit these MLRs. These data suggested that IL-16 and IL-10 acted additively to inhibit MLR.

3.2. Production and MLR inhibition of IL-16 and IL-10 secreted from a human skin keratinocyte-equivalent model, OSC-20 cells

The above data led us to develop a model of tolerogenic human skin substitute which produced IL-16 and IL-10. To this end, we used the human squamous cancer cell line OSC-20 as a model for the skin keratinocytes. We previously made the human IL-16-cDNA-transfected OSC-20 cell clone, OSC-20-IL16#4, which secreted 50 ng/ml of IL-16, and control plasmid (pcDSRα-E3 without IL-16-cDNA)-transfected OSC-20 cells, OSC-20-pcDSRα [4]. OSC-20-IL16#4 cells were transfected with a mixture of plasmids pLXSN-IL-10 and maintained in puromycin- and geneticin-containing medium. Several clones were obtained, and IL-10 production in the culture supernatant was determined by colorimetric ELISA. As a control, we used a mixture of plasmids pcDSRα-E3, pBabe Puro and pLXSN. We confirmed the insertion of the IL-10 gene by sequencing reverse transcriptase PCR products in all of transfectants #6 and #7 (data not shown). As depicted in Fig. 2A, it appeared that the OSC-20-IL16IL10#6 transfectant clone was the highest producer of IL-10 among selected transfectant clones OSC-20-IL16IL10#6 and #7. However, it seemed that the amounts of IL-16 production by each of these transfectants were the same, except for the control (Fig. 2B).

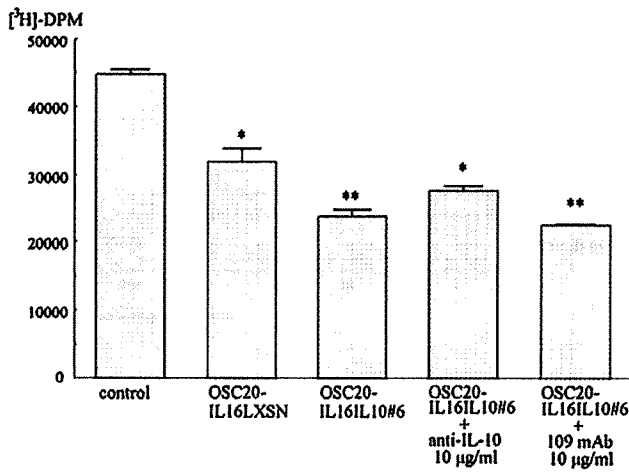


Fig. 3 – Inhibition of human mixed lymphocyte reaction by the supernatant of IL-16- and IL-10-producing OSC-20 clone. Bars represent ±standard error. **p* < 0.05 and *p* < 0.01.**

By using the supernatant of an IL-16 and IL-10 double-producer clone, OSC-20-IL16IL10#6, we then assessed whether it could inhibit MLR. The responder lymphocytes were treated with the culture supernatant and mixed with mitomycin-C-treated stimulator cells. The reactivity of responder lymphocytes was then analysed as described above. As shown in Fig. 3, the supernatant of the transfectant clone OSC-20-IL16IL10#6, the highest IL-16 and IL-10 double-producer, inhibited MLR most efficiently. Inhibition was cancelled selectively only when anti-IL-10 mAb (IgG1) was added to the MLR assay, whereas isotype (IgG1)-matched control 109 mAb could not cancel the inhibition, compared with the inhibition of MLR by the supernatant of OSC-20-IL16pLXSN which secreted IL-16 only. These data indicated that the supernatant of transfectant clone OSC-20-IL16IL10#6 could inhibit MLR most strongly, because of the additive effect of secreted IL-16 and IL-10.

3.3. Direct MLR inhibition by IL-16- and IL-10-cDNA-double-transfected OSC-20 lines with T cells

Finally, we determined the direct interaction between allogeneic lymphocytes and transfected OSC-20 cells. In this experiment, the control plasmid (pcDSRα-E3 and pLXSN)-transfected OSC-20 (control), pcDSRα-E3-IL16 and pLXSN-transfected OSC-20 (OSC-20-IL16pLXSN) and pcDSRα-E3-IL16- and pLXSN-IL10-transfected OSC-20 cells (OSC-20-IL16IL10#6) as stimulator cells were irradiated with 6000 rad, and allogeneic lymphocytes (HLA-haplotype: HLA-A2, A33, B17, B61, Cw3, DR6) were added as the responder. Using colorimetric ELISA, we confirmed that OSC-20-IL16IL10#6 continued to release IL-16 and IL-10 after they had been irradiated (data not shown).

As depicted in Fig. 4A, OSC-20-IL16IL10#6 cells inhibited this MLR most strongly when compared with control cells and OSC-20-IL16pLXSN. In the direct MLR assay, the effects appeared to be irrelevant to the MHC class I expres-

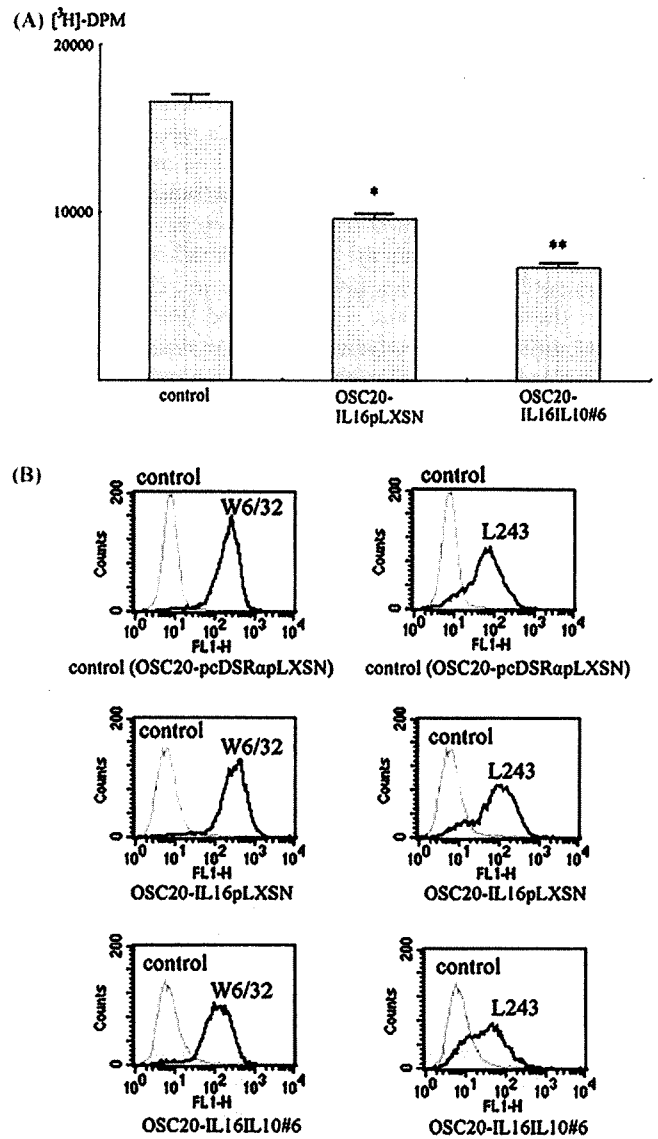


Fig. 4 – (A) Inhibition of the reactivity of allogeneic lymphocytes with IL-16- and IL-10-producing OSC-20 clone. Bars represent ±standard error. **p* < 0.05 and *p* < 0.01. (B) Fluorescence-activated cell sorter (FACS) profile of the expression of major histocompatibility complex class I and class II molecules of OSC-20 transfectants as determined by W6/32 mAb and L243 mAb, respectively. Control denotes the FACS pattern of cells stained without W6/32 or L243.**

sion on the cell surface as assessed by MHC class I-specific W6/32 mAb. However, they appeared to be relevant to the MHC class II expression on the cell surface, since IL-10-producing OSC-20-IL16IL10#6 cells exhibited a down-regulation of MHC class II expression as assessed by MHC class II-specific L243 mAb (Fig. 4B). Taken together, these data indicated that IL-16- and IL-10-double-producing allogeneic squamous cells, which are considered skin keratinocyte equivalents, work as direct inhibitors of allogeneic lymphocyte activation.

4. Discussion

Although many synthetic skin substitutes have been produced [13-15], the mainstay of treatment for extensive severe burns is still transplantation of skin allografts. However, the therapeutic effect of these grafts ceases with their immunological rejection. Therefore, prolongation of skin allograft survival has been a major aim of clinical treatment. It is recognised that in the field of allogeneic organ transplantations it is relatively difficult to delay the immunological rejection of skin. Perhaps these phenomena may have something to do with the ample presence of MHC class II-positive professional antigen-presenting cells, such as dermal dendritic cells, in the skin. Furthermore, certain epidermal keratinocytes express MHC class II antigen on the cell surface as well [16]. These characteristics indicate that the prolongation of skin allograft survival may require a more potent additional therapeutic regimen.

In the *in vitro* studies, anti-rat CD4 mAb RTH7 [17,18] significantly reduced rat allogeneic MLR (data not shown). In our study, however, this mAb prolonged *in vivo* skin allograft survival only minimally. This might be due to antibody neutralisation and rapid clearance *in vivo* or to insufficient delivery of mAb to the skin tissue. We previously assessed the effect of topically applied 0.5% FK506 ointment in the rat skin allograft model. The treatment was clearly effective for local immunosuppression and consequent delay of skin allograft rejection by up to 1 week compared with placebo treatment, even though the blood concentration of FK506 was mostly below levels detectable by ELISA with a mouse anti-FK506 monoclonal antibody [19]. From the same point of view, we speculate that an efficient way to prolong skin allograft survival might be to develop an *in situ* immunosuppressive mechanism in the skin. Thus, we planned the experiment in which the cytokines inhibiting MLR were one of the *in situ* immunosuppressive agents.

IL-16 was first described in 1982 as a lymphocyte chemoattractant factor generated by mitogen-stimulated human peripheral mononuclear cells [20]. The functional bioactivities of IL-16 towards CD4 T cells involve the migration and upregulation of surface-expressed IL-2 receptor, the G0 to G1 transition of the cell cycle and increased cell growth [21]. On the other hand, it was also reported that IL-16 acted as the natural ligand of the CD4 molecule and inhibited MLR, although it did not influence MHC class II expression on the cell surface [22].

Meanwhile, IL-10 has been identified as a cytokine synthesis inhibitory factor capable of suppressing the production of Th1 cytokines including IL-2 and IFN- γ [23-26]. In addition, IL-10 inhibits the production of most cytokines produced by monocytes/macrophages [27,28] and polymorphonuclear neutrophils [29,30]. IL-10 also strongly reduces antigen-specific T cell proliferation by diminishing the antigen-presenting capacity of monocytes via down-regulation of MHC class II expression [31]. Because IL-10 is well known as an immunosuppressive cytokine, attempts have been made to more thoroughly investigate its function in a number of *in vivo* models including endotoxemia [32-36], transplantation [37-39], autoimmune diseases [40], diabetes in non-obese mice [41] and allergen-induced lung inflammation [42].

In this study, we demonstrated that IL-16 enhanced or added independently to the immunosuppressive effect of IL-10 in allogeneic MLR. It was therefore concluded that if the

skin equivalent was reconstituted with skin cells which secreted both IL-16 and IL-10, it might induce the most efficient local immunosuppressive effect and so prolong skin allograft survival. It is known that skin keratinocytes express MHC class II molecules on the cell surface [16], and allogeneic skin graft rejection will be triggered by the interaction of dendritic cells, MHC class II-positive keratinocytes and lymphocytes. Thus we compared the immunosuppressive effects of IL-16 and IL-10 on the MLR between responder lymphocytes and MHC class II-positive skin keratinocyte-equivalent cells, such as the OSC-20 line.

We transfected the IL-16 and IL-10 expression vector to OSC-20, and IL-16- and IL-10-double-producing OSC-20 clones were obtained. Consequently IL-16 and IL-10, secreted in the culture supernatant of these clones, inhibited MLR most significantly. Furthermore, the reactivity of allogeneic lymphocytes directly cultured with these OSC-20 clones was also inhibited. It was confirmed that the MHC class II expression on the cell surface of these OSC-20 clones was down-regulated. Such observations have previously been reported in the literature [43-48] and may be due to the biological effects of the secreted IL-10. Our results suggest that the inhibition of allogeneic lymphocyte reactivity might be due to direct action of secreted IL-16 and IL-10, and indirect action through down-regulation of MHC class II expression by the secreted IL-10. Taken together, our results suggest that, in clinical practice, gene therapy based on the introduction of IL-16-cDNA and IL-10-cDNA to the skin cells might confer the capability of prolonging survival of this allogeneic skin substitute.

Transfection to normal cells *in vivo* by methods such as a gene gun with naked DNA, or an adenovirus vector, is not stable; it is predicted that the amount of cytokines secreted from the transfectants would decrease or the transfected gene expression itself would disappear. Therefore, if the current transfection method is used, it seems difficult for differentiated skin cells to achieve the concentrations of cytokines secreted by *in vitro* cell lines. Normal human keratinocyte culture is usually maintained only up to passages 6-8, and it is difficult for these cells to be stably transfected with double-cDNA. However, normal human fibroblasts can be maintained up to passage 50 at least, so we think a stable double transfection can be achieved in primary fibroblasts. Moreover, if normal human keratinocytes are immortalised by the transfection with genes such as hTERT, we think that stable double transfection could be achieved in this cell line as well.

We consider that normal keratinocytes and fibroblasts harvested from allogeneic skin can be stably transfected with immunosuppressive cytokine cDNA *in vitro* and then the allogeneic skin equivalent could be reconstituted from these stable transfectants, which would maintain high amounts of cytokine secretion. These cells could be transplanted to severe burns as allografts. To this end we are now studying the *in vivo* effects of IL-16- and IL-10-cDNA-double-transfected skin cells.

Acknowledgement

This work was supported by a Research Grant for Immunology, Allergy, and Organ Transplant, from the Ministry of Health and Welfare, Japan.

REFERENCES

- [1] Brown JB, Minot PF, Randall P. Postmortem homograft as "biological dressing" for extensive burns and denuded areas. *Ann Surg* 1953;138:618-29.
- [2] Zaroff LI, Mills W, Duckett JW, Switzer WE, Moncrief JA. Multiple uses of viable cutaneous homografts in the burned patient. *Surgery* 1966;59:368-72.
- [3] Spence RJ, Wong L. The enhancement of wound healing with human skin allograft. *Surg Clin North Am* 1977;77:731-45.
- [4] Fujita T, Matsumoto Y, Hirai I, Ezoe K, Saito T, Yagihashi A, et al. Immunosuppressive effect on T cell activation by interleukin-16-cDNA-transfected human squamous cell line. *Cell Immunol* 2000;202:54-60.
- [5] Bejarano MT, de Waal Malefyt R, Abrams JS, Bigler M, Bacchetta R, de Vries JE, et al. IL-10 inhibits allogeneic proliferative and cytotoxic T cell responses generated in primary MLR. *Int Immunol* 1992;4:1389-97.
- [6] Miyazaki A, Sato N, Takahashi S, Sasaki A, Kohama G, Yamaguchi A, et al. Cytotoxicity of histocompatibility leukocyte antigen-DR8-restricted CD4+ killer T cells against human autologous squamous cell carcinoma. *Jpn J Cancer Res* 1997;88:191-7.
- [7] Yokoi T, Hirata S, Nishimura F, Miyakawa A, Odajima T, Kohama G, et al. Some properties of a newly established human cell line derived from an oral squamous carcinoma. *Tumor Res* 1990;25:93-103.
- [8] Morgenstein JP, Land H. Advanced mammalian gene transfer; high titer retroviral vectors with multiple drug selection markers and a complementary helper-free packaging cell line. *Nucleic Acids Res* 1990;18:3587-96.
- [9] Cho JM, Sato N, Yagihashi A, et al. Natural killer target molecules associated with the transformation of the oncogene-transformed fibroblast. *Cancer Res* 1991;51:4250-6.
- [10] Brodsky FM, Bodmer WF, Parham P. Characterization of a monoclonal anti-beta 2-microglobulin antibody and its use in the genetic and biochemical analysis of major histocompatibility antigens. *Eur J Immunol* 1979;9:536-45.
- [11] Smith LM, Petty HR, Parham P, McConnell HM. Cell surface properties of HLA antigens on Epstein-Barr virus-transformed cell lines. *Proc Natl Acad Sci USA* 1982;79:608-12.
- [12] Moore KW, O'Garra A, de Waal Malefyt R, Vieira P, Mosmann TR. Interleukin-10. *Annu Rev Immunol* 1993;11:165-90.
- [13] Peters WJ. Biological dressings in burns—a review. *Ann Plast Surg* 1980;4:133-7.
- [14] Alexander JW, Wheeler LM, Rooney RC, McDonald JJ, MacMillan BG. Clinical evaluation of epigard, a new synthetic substitute for homograft and heterograft skin. *J Trauma* 1973;13:374-83.
- [15] Friedman SJ, Su WPD. Management of leg ulcers with hydrocolloid occlusive dressing. *Arch Dermatol* 1984;120:1329-36.
- [16] Albanesi C, Cavani A, Girolomoni G. Interferon- γ stimulated human keratinocytes express the genes necessary for the production of peptide-loaded MHC class II molecules. *J Invest Dermatol* 1988;110:138-42.
- [17] Tamura Y, Tsuboi N, Sato N, Kikuchi K. 70 kDa heat shock cognate protein is a transformation-associated antigen and a possible target for the host's anti-tumor immunity. *J Immunol* 1993;151:5516-24.
- [18] Yamaki T, Uede T, Shijubo N, Kikuchi K. Functional analysis of mononuclear cells infiltrating into tumors. III. Soluble factors involved in the regulation of T lymphocyte infiltration into tumors. *J Immunol* 1988;140:4388-96.
- [19] Fujita T, Takahashi S, Yagihashi A, Jimbow K, Sato N. Prolonged survival of rat skin allograft by treatment with FK506 ointment. *Transplantation* 1997;64:922-5.
- [20] Cruikshank WW, Kornfeld H, Center DM. Signaling and functional properties of interleukin-16. *Int Rev Immunol* 1988;16:523-40.
- [21] Cruikshank WW, Center DM, Nisar N, Wu M, Natke B, Theodore AC, et al. Molecular and functional analysis of a lymphocyte chemoattractant factor; association of biological function with CD4 expression. *Proc Natl Acad Sci USA* 1994;91:5109-13.
- [22] Theodore AC, Center DM, Nicoll J, Fine G, Kornfeld H, Cruikshank WW. CD4 ligand IL-16 inhibits the mixed lymphocyte reaction. *J Immunol* 1996;59:1958-64.
- [23] Fiorentino DF, Bond MW, Mosmann TR. Two types of mouse T helper cell. IV. Th2 clones secrete a factor that inhibits cytokine production by Th1 clones. *J Exp Med* 1989;170:2081-95.
- [24] Vieira P, de Waal-Malefyt R, Dang MN, Johnson KE, Kastelein R, Fiorentino DF, et al. Isolation and expression of human cytokine synthesis inhibitory factor cDNA clones: homology to Epstein-Barr virus open reading frame BCRF1. *Proc Natl Acad Sci USA* 1991;88:1172-6.
- [25] Fiorentino DF, Zlotnik A, Vieira P, Howard M, O'Garra A. IL-10 acts on the antigen-presenting cell to inhibit cytokine production by Th1 cells. *J Immunol* 1991;146:3444-51.
- [26] Taga K, Tosato G. IL-10 inhibits human T cell proliferation and IL-2 production. *J Immunol* 1992;148:1143-8.
- [27] de Waal Malefyt R, Abrams J, Bennet B, Figdor CG, de Vries JE. Interleukin 10 (IL-10) inhibits cytokine synthesis by human monocytes: an autoregulatory role of IL-10 produced by monocytes. *J Exp Med* 1991;174:1209-20.
- [28] Fiorentino DF, Zlotnik A, Mosmann TR, Howard M, O'Garra A. IL-10 inhibits cytokine production by activated macrophages. *J Immunol* 1991;147:3815-22.
- [29] Cassatella MA, Meda L, Bonora S, Ceska M, Constantin G. Interleukin 10 (IL-10) inhibits the release of proinflammatory cytokines from human polymorphonuclear leukocytes. Evidence for an autocrine role of tumor necrosis factor and IL-1 β in mediating the production of IL-8 triggered by lipopolysaccharide. *J Exp Med* 1993;178:2207-11.
- [30] Kasama T, Strieter RM, Lukacs NW, Burdick MD, Kunkel SL. Regulation of neutrophil derived chemokine expression by IL-10. *J Immunol* 1994;152:3559-69.
- [31] de Waal-Malefyt R, Haanen J, Spits H, Roncarolo MG, te Velde A, Figdor C, et al. Interleukin 10 (IL-10) and viral IL-10 strongly reduce antigen-specific human T cell proliferation by diminishing the antigen-presenting capacity of monocytes via downregulation of class II major histocompatibility complex expression. *J Exp Med* 1991;174:915-24.
- [32] Drazan KE, Wu L, Bullington D, Shaked A. Viral IL-10 gene therapy inhibits TNF- α and IL-1 β , not IL-6, in the newborn endotoxemic mouse. *J Pediatr Surg* 1996;31:411-4.
- [33] Xing Z, Ohkawara Y, Jordana M, Graham FL, Gaudie J. Adenoviral vector-mediated interleukin-10 expression in vivo: intramuscular gene transfer inhibits cytokine responses in endotoxemia. *Gene Ther* 1997;4:140-9.
- [34] Gerard C, Bruyns C, Marchant A, Abramowicz D, Vandenaabeele P, Delvaux A, et al. Interleukin 10 reduces the release of tumor necrosis factor and prevents lethality in experimental endotoxemia. *J Exp Med* 1993;177:547-50.
- [35] Pajkrt D, Camoglio L, Tiel-van Buul MC, de Bruin K, Cutler DL, Affrime MB, et al. Attenuation of proinflammatory responses by recombinant human IL-10 in human endotoxemia. *J Immunol* 1997;158:3971-7.

- [36] Van der Poll T, Jansen PM, Montegut WJ, Braxton CC, Calvano SE, Stackpole SA, et al. Effects of IL-10 on systemic inflammatory responses during sublethal primate endotoxemia. *J Immunol* 1997;158:1971-5.
- [37] Suzuki T, Tahara H, Narula S, Moore KW, Robbins PD, Lotze MT. Viral interleukin-10 (IL-10), the human herpes virus 4 cellular IL-10 homologue, induces local anergy to allogeneic and syngeneic tumors. *J Exp Med* 1995;182:477-86.
- [38] Qin L, Chavin KD, Ding Y, Tahara H, Favaro JP, Woodward JE, et al. Retrovirus-mediated transfer of viral IL-10 gene prolongs murine cardiac allograft survival. *J Immunol* 1996;156:2316-23.
- [39] Zheng XX, Steele AW, Nickerson PW, Steurer W, Steiger J, Strom TB. Administration of noncytolytic IL-10/Fc in murine models of lipopolysaccharide-induced septic shock and allogeneic islet transplantation. *J Immunol* 1995;154:5590-600.
- [40] Mathisen PM, Yu M, Johnson JM, Drazba JA, Tuohy VK. Treatment of experimental autoimmune encephalomyelitis with genetically modified memory T cells. *J Exp Med* 1997;186:159-64.
- [41] Zheng XX, Steele AW, Hancock WW, Stevens AC, Nickerson PW, Roy-Chaudhury P, et al. A noncytolytic IL-10/Fc fusion protein prevents diabetes, blocks autoimmunity, and promotes suppressor phenomena in NOD mice. *J Immunol* 1997;158:4507-13.
- [42] Grunig G, Corry DB, Leach MW, Seymour BWP, Kurup VP, Rennick DM. Interleukin-10 is a natural suppressor of cytokine production and inflammation in a murine model of allergic bronchopulmonary aspergillosis. *J Exp Med* 1997;185:1089-99.
- [43] Kooy AJ, Prens EP, van Heukelum A, Vuzevski VD, van Joost T, Tank B. Interferon- γ -induced ICAM-1 and CD40 expression, complete lack of HLA-DR and CD80 (B7.1), and inconsistent HLA-ABC expression in basal cell carcinoma: a possible role for interleukin-10? *J Pathol* 1999;187:351-7.
- [44] Redpath S, Angulo A, Gascoigne NR, Ghazal P. Murine cytomegalovirus infection down-regulates MHC class II expression on macrophages by induction of IL-10. *J Immunol* 1999;162:6701-7.
- [45] Chadban SJ, Tesch GH, Foti R, Lan HY, Atkins RC, Nikolic-Paterson DJ. Interleukin-10 differentially modulates MHC class II expression by mesangial cells and macrophages in vitro and in vivo. *Immunology* 1998;94:72-8.
- [46] Koppelman B, Neefjes JJ, de Vries JE, de Waal Malefyt R. Interleukin-10 down-regulates MHC class II alphabeta peptide complexes at the plasma membrane of monocytes by affecting arrival and recycling. *Immunity* 1997;7:861-71.
- [47] Boorstein SM, Elnor SG, Bian ZM, Strieter RM, Kunkel SL, Elnor VM. Selective IL-10 inhibition of HLA-DR expression in IFN-gamma-stimulated human retinal pigment epithelial cells. *Curr Eye Res* 1997;16:547-55.
- [48] Yue FY, Dummer R, Geertsen R, Hofbauer G, Laine E, Manolio S, et al. Interleukin-10 is a growth factor for human melanoma cells and down-regulates HLA class-I, HLA class-II and ICAM-1 molecules. *Int J Cancer* 1997;71:630-7.

Scythe/BAT3 regulates apoptotic cell death induced by papillomavirus binding factor in human osteosarcoma

Tomohide Tsukahara,^{1,2,3,4} Shigeharu Kimura,^{1,2,3} Shingo Ichimiya,¹ Toshihiko Torigoe,¹ Satoshi Kawaguchi,² Takuro Wada,² Toshihiko Yamashita² and Noriyuki Sato¹

¹Department of Pathology, Sapporo Medical University School of Medicine, South-1, West-17, Chuo-ku, Sapporo 060-8556; ²Department of Orthopaedic Surgery, Sapporo Medical University School of Medicine, South-1, West-16, Chuo-ku, Sapporo 060-8543, Japan

(Received March 20, 2008/Revised August 27, 2008/Accepted September 4, 2008/Online publication October 30, 2008)

Papillomavirus binding factor (PBF) was first identified as a transcription factor regulating the promoter activity of human papillomavirus. We previously demonstrated that PBF is an osteosarcoma-associated antigen and 92% of osteosarcoma tissues express PBF in the nucleus. Moreover, PBF-positive osteosarcoma has a significantly poorer prognosis than that with negative expression of PBF. In the present study, we assessed the biological role of PBF in cell survival. Overexpression of PBF induced cell death-mediated lactate dehydrogenase (LDH) release from 293EBNA cells. Cleaved poly(ADP-ribose) polymerase and active caspase-3 were also detected. However, PBF-induced apoptosis did not affect caspase-9 activity. Next, to identify the apoptosis regulator of PBF, we screened a cDNA library constructed from mRNA of the osteosarcoma cell line OS2000 using a yeast two-hybrid system and isolated Scythe/BAT3. Scythe/BAT3 mRNA was detected in 56% of osteosarcoma tissues and ubiquitously in various normal tissues. Although Scythe/BAT3 was localized to the cytoplasm in normal tissue, it was localized to the nucleus in osteosarcoma tissue. PBF and Scythe/BAT3 also colocalized to the cytoplasm in 293T cells and the nucleus in OS2000. Furthermore, overexpression of Scythe/BAT3 suppressed cell death events that resulted from overexpression of PBF in OS2000, but not in 293EBNA cells. Thus, our results support the ideas that: (i) PBF could induce apoptotic cell death via a caspase-9-independent pathway; (ii) the apoptosis regulator Scythe/BAT3 is a PBF-associated molecule acting as a nucleus-cytoplasm shuttling protein; and (iii) colocalization of PBF and Scythe/BAT3 in the nucleus might be an important factor for survival of osteosarcoma cells. (*Cancer Sci* 2009; 100: 47–53)

Papillomavirus binding factor (PBF) was first identified as a transcription factor regulating promoter activity of the human papillomavirus type 8 genome.⁽¹⁾ We demonstrated that PBF is an osteosarcoma-associated antigen recognized by an autologous cytotoxic T lymphocyte clone.⁽²⁾ Immunohistochemical analysis revealed that 92% of biopsy specimens of osteosarcoma express PBF. Moreover, PBF-positive osteosarcoma has a significantly poorer prognosis than that with negative expression of PBF.⁽³⁾ Generally, conventional osteosarcoma is a malignant neoplasm of mesenchymal origin and there is no specific cause such as viral infection.⁽⁴⁾ Therefore, it is suggested that PBF has certain functions not only in transcription of the human papillomavirus genome, but also in the cell survival and apoptosis of osteosarcoma.

Apoptosis is tightly controlled programmed cell death. Generally, it is induced by two major pathways, an extrinsic pathway and an intrinsic pathway.⁽⁵⁾ The initiation of the extrinsic pathway of apoptosis is triggered by extracellular death signals. The binding of extracellular ligands to the death receptors of the tumor necrosis factor receptor superfamily leads to formation

of the death-inducing signaling complex, which is capable of activating the initiator caspase-8.^(6–8) Meanwhile, initiation of the intrinsic pathway of apoptosis is triggered by cellular stress. Cellular death signals induce mitochondrial membrane permeabilization, mitochondrial cytochrome *c* release and activation of the initiator caspase-9.^(5,8,9) Apart from these two major pathways, mitochondrial membrane permeabilization also leads to the release of apoptosis-inducing factor (AIF), which induces caspase-independent cell death.⁽¹⁰⁾ Recently, Sichtig *et al.* reported that PBF is an inducer of cell death and that 14-3-3 regulates the localization of PBF and PBF-induced cell death in skin keratinocytes.⁽¹¹⁾ 14-3-3 is associated with apoptotic cell death, the cell cycle, and regulation of various oncogenes and tumor-suppressor genes.^(12,13) Moreover, 14-3-3 binds to the Bcl-2 family member Bax and inhibits Bax-induced cytochrome *c* release from the mitochondria upon apoptotic stimuli.⁽¹⁴⁾ Although these findings suggest a certain function of PBF as an apoptosis regulator, the function of PBF in osteosarcoma cells remains unknown.

In the present study, we demonstrated that PBF-induced cell death results from apoptosis via a caspase-9-independent pathway. Next, we identified Scythe/BAT3^(15,16) as a PBF-associated molecule using a yeast two-hybrid system. Finally, we showed that PBF-induced apoptotic cell death is inhibited by Scythe/BAT3 colocalized to the nuclei of osteosarcoma cells. Taken together, these findings suggest that both PBF and Scythe/BAT3 might play important roles in apoptosis of osteosarcoma cells.

Materials and Methods

The present study was approved under institutional guidelines for the use of human subjects in research. The patients and their families gave informed consent for the use of tissue specimens in our research.

Cell lines. The osteosarcoma cell lines OS2000, HOS, Saos-2, and U2OS, as well as the human embryonic kidney cell lines 293EBNA and 293T, were used. 293EBNA and 293T cells did not express endogenous PBF protein (data not shown). OS2000 was established in our laboratory.⁽¹⁷⁾ The other cell lines were purchased from American Type Culture Collection (Manassas, VA, USA).

Antibodies. The mouse monoclonal antibodies used in the present study were anti-cleaved poly(ADP-ribose) polymerase (PARP) (D216, 1:1000 dilution; Cell Signaling, Danvers, MA,

³These authors contributed equally to this work.

⁴To whom correspondence should be addressed. E-mail: tsukahara@sapmed.ac.jp

USA), anti-caspase-9 (clone 5B4, :1000 dilution; MBL International, Woburn, MA, USA), anti- β -actin (clone AC-15, 1:1000 dilution; Sigma-Aldrich, St Louis, MO, USA), anti-myc (clone 9E10, 1:1000 dilution; American Type Culture Collection), and anti-human influenza hemagglutinin (HA) (HA-7, 1:10 000 dilution and 1:2000 in western blotting and immunofluorescence analysis, respectively; Sigma-Aldrich, St Louis, MO, USA). Rabbit polyclonal antibodies used were anti-Scythe/BAT3, kindly provided by Dr Peter J. McKinnon (St Jude Children's Research Hospital, Minneapolis, TN, USA; #23, used at 1:8000 dilution and 1:200 in western blotting and immunofluorescence analysis, respectively),⁽¹⁸⁾ and anti-PBF (used at 1:800 dilution and 1:200 in western blotting and immunofluorescence analysis, respectively; SigmaGenosys, Sapporo, Japan).⁽²⁾

Screening of a cDNA library using the yeast two-hybrid system.

A cDNA library was constructed from OS2000 mRNA using a FastTrack 2.0 mRNA Isolation Kit (Invitrogen, Carlsbad, CA, USA) and the Superscript Choice System (Invitrogen). The cDNA was ligated to *EcoRI*-*XhoI* adapters and digested with *XhoI*. The resultant cDNA was cloned into the pACT2 vector (Clontech Laboratories, Mountain View, CA, USA). Recombinant plasmids were electroporated into Electromax DH10B cells (Invitrogen) and selected with ampicillin (100 μ g/mL). The resultant 30 000 clones were amplified and plasmid DNA was extracted using a Qiagen Plasmid Maxi Kit (Qiagen, Hilden, Germany). Full-length PBF subcloned into the pGBKT7 vector (Clontech) was used as bait to screen the cDNA library. Screening of the cDNA library was carried out according to the Mammalian Matchmaker Two-hybrid Assay Kit protocol (Clontech).

Reverse transcription-polymerase chain reaction analysis. Expression of Scythe/BAT3 was determined by reverse transcription-polymerase chain reaction (PCR). Normal-tissue cDNA was purchased (Multiple Tissue cDNA Panels; Clontech). Total RNA was extracted from nine osteosarcoma biopsy specimens and reverse transcribed. PCR was carried out with KOD dash DNA polymerase (Toyobo, Tokyo, Japan), using the forward primer (*XhoI*-Scythe/BAT3-FW) 5'-GGGGGGCTCG-AGAAATGGAGCCTAATGATAGTACCAGT-3' and the reverse primer (Scythe/BAT3-NotI-Rv) 5'-AAAAAAGCGCCGCC-TAAGGATCATCAGCAAAGGCCCGC-3'. The mixture was denatured at 98°C for 2 min, followed by 30 cycles at 98°C for 15 s, 56°C for 2 s, and 74°C for 3 min. Reaction products were analyzed by electrophoresis on 1.0% agarose gels with ethidium bromide. Full-length Scythe/BAT3 cDNA, amplified from OS2000 cDNA by PCR, was digested with *XhoI* and *NotI* and subcloned into the pCMV-HA tag vector (Clontech).

Transfection. 293EBNA or 293T cells were transfected with the indicated cDNA or small interfering RNA (siRNA) using Lipofectamine 2000 (Invitrogen) in Dulbecco's modified Eagle's medium containing 10% fetal calf serum in six-well plates according to the manufacturer's protocol. OS2000 or U2OS cells were transfected with cDNA using Cell Line Nucleofector Kit V (Amaxa, Cologne, Germany) according to the manufacturer's protocol.

Western blotting. Cell lines and biopsy specimens were homogenized and suspended in ice-cold Nonidet P-40 (NP-40) buffer for 20 min as described previously.⁽¹⁹⁾ The lysates were mixed with 2 \times sample buffer and boiled for 5 min. Then the lysates were separated by sodium dodecylsulfate-polyacrylamide gel electrophoresis (SDS-PAGE) on 7 or 13% gels and transferred to polyvinylidene fluoride membranes (Millipore, Billerica, MA, USA). The membranes were blocked and probed with the indicated antibodies for 40 min at room temperature. The membranes were then stained with peroxidase-labeled secondary antibody and visualized using an enhanced chemiluminescence detection system (Amersham Life Science, Arlington Heights, IL, USA).

Silencing of Scythe/BAT3. Three Stealth siRNA targeting Scythe/BAT3 and a negative control siRNA were purchased from

Invitrogen. Three micrograms of each siRNA was transfected into 293EBNA cells and OS2000 cells as described above. After screening of their silencing effect using western blotting (data not shown), one of the three siRNA (BAT3-HSS111846) was selected for further analysis.

Immunoprecipitation. The cells were lysed on ice with NP-40 lysis buffer. Lysates were precleared with protein A-sepharose beads (Phadia, Uppsala, Sweden) before immunoprecipitation. The anti-HA-7 monoclonal antibody and aliquots of lysates were mixed and incubated at 4°C for 24 h. Immunoprecipitates were recovered from the mixture using protein A-sepharose beads, washed three times with phosphate-buffered saline (PBS) containing 0.1% NP-40, mixed with SDS-PAGE gel electrophoresis running buffer, and boiled for 5 min. Supernatants containing immunoprecipitates were fractionated on 13% SDS-PAGE, dried, and exposed to X-ray films with an intensifying screen.

Immunofluorescence analysis. OS2000, U2OS and 293T cells cultured on glass coverslips (Asahi Techno Glass, Tokyo, Japan) were fixed in 4% paraformaldehyde and permeabilized in 0.1% Triton X-100. After washing with PBS, cells were incubated with the polyclonal anti-PBF antibody and monoclonal anti-HA antibody to detect the subcellular localization of PBF protein and HA-tagged Scythe/BAT3 protein. The monoclonal anti-myc antibody and polyclonal anti-Scythe/BAT3 antibody were used to detect exogenous myc-tagged PBF protein and endogenous Scythe/BAT3 protein. 4',6-Diamidino-2'-phenylindole dihydrochloride (DAPI) was used for counterstaining nuclei. After washing with PBS, cells were immunostained with secondary antibodies (Alexa Fluor 488- or Alexa Fluor 594-conjugated goat anti-mouse or anti-rabbit antibodies; Invitrogen). After staining, cells were visualized by confocal laser microscopy (R2100AG2; Bio-Rad Laboratories, Hercules, CA, USA). Formalin-fixed paraffin-embedded sections of one osteosarcoma biopsy specimen and autopsy specimens of liver, pancreas, and kidney (obtained from a brain infarction patient) were deparaffinized and incubated with the polyclonal anti-Scythe/BAT3 antibody overnight at 4°C. After washing with PBS, cells were immunostained with Alexa Fluor 488-conjugated goat anti-rabbit IgG, followed by visualization using confocal laser microscopy. DAPI was used for counterstaining of nuclei.

Lactate dehydrogenase (LDH) release assay. 293EBNA, 293T or OS2000 cells were transfected with cDNA as described above. After a 24-h incubation period at 37°C, the supernatant was replaced with AIM-V. The amount of LDH in the supernatant was measured by colorimetric assay using an LDH Cytotoxicity Detection Kit (Takara, Ohtsu, Japan) after an additional 24 h incubation period. LDH release was calculated using the following equation: LDH release = ([sample release] - [spontaneous release]).

Caspase-3 colorimetric assay. 293EBNA cells were transfected with cDNA as described above. After a 24-h incubation period at 37°C, the amount of active caspase-3 in the supernatant was measured by colorimetric assay using an APOPCYTO Caspase-3 Colorimetric Assay Kit (Medical and Biological Laboratories, Nagoya, Japan) according to the manufacturer's protocol.

Statistical analysis. Significant differences among samples in the LDH release assay and caspase-3 colorimetric assay were determined by Welch's *t*-test using StatMate III for Macintosh v3.10 (ATMS, Tokyo, Japan). A probability of less than 0.05 was considered statistically significant.

Results

Overexpression of PBF induces apoptotic cell death via a caspase-independent pathway. To investigate the function of PBF as an apoptosis regulator, we analyzed the cell death and apoptotic events that occurred in 293EBNA cells transfected transiently with PBF. As shown in Figure 1a, overexpression of PBF induced cell death-mediated LDH release from 293EBNA and